AGU PUBLICATIONS

Tectonics

RESEARCH ARTICLE
10.1002/2015TC003861

Key Points:
- We present new MCS and bathymetry of the NW Algero-Balearic basin
- The NW Algero-Balearic margin formed by middle-late Miocene volcanic accretion
- Volcanic highs are NE-SW anticlines produced by late Miocene NW-SE shortening

Supporting Information:
- Supporting Information S1

Correspondence to:
F. Giaconia,
giaconia.flavio@gmail.com

Citation:
Giaconia, F., et al. (2015), Compressional tectonic inversion of the Algero-Balearic basin: Latemost Miocene to present oblique convergence at the Palomares margin (Western Mediterranean), *Tectonics*, *34*, 1516–1543, doi:10.1002/2015TC003861.

Received 16 FEB 2015
Accepted 7 MAY 2015
Accepted article online 12 MAY 2015
Published online 30 JUL 2015

Compressional tectonic inversion of the Algero-Balearic basin: Latemost Miocene to present oblique convergence at the Palomares margin (Western Mediterranean)

Flavio Giaconia[1], Guillermo Booth-Rea[1], César R. Ranero[2], Eulàlia Gràcia[3], Rafael Bartolome[3], Alcinoe Calahorrano[3], Claudio Lo Iacono[4], Montserrat G. Vendrell[3], Alejandra L. Cameselle[3], Sergio Costa[3], Laura Gómez de la Peña[3], Sara Martínez-Loriente[3], Hector Perea[3], and Marina Viñas[3]

[1]Departamento de Geodinámica, Instituto Andaluz de Ciencias de la Tierra (CSIC-UGR), Granada, Spain, [2]Barcelona Center for Subsurface Imaging, ICREA at CSIC, Institut de Ciències del Mar, Barcelona, Spain, [3]Barcelona Center for Subsurface Imaging, Institut de Ciències del Mar, CSIC, Barcelona, Spain, [4]Marine Geoscience, National Oceanography Centre, Southampton, UK

Abstract Interpretation of new multichannel seismic reflection profiles indicates that the Palomares margin was formed by crustal-scale extension and coeval magmatic accretion during middle to late Miocene opening of the Algero-Balearic basin. The margin formed at the transition between thinned continental crust intruded by arc volcanism and back-arc oceanic crust. Deformation produced during the later positive inversion of the margin offshore and onshore is partitioned between ~N50°E striking reverse faults and associated folds like the Sierra Cabrera and Abubacer anticlines and N10–20°E sinistral strike-slip faults like Palomares and Terreros faults. Parametric subbottom profiles and multibeam bathymetry offshore, structural analysis, available GPS geodetic displacement data, and earthquake focal mechanisms jointly indicate that tectonic inversion of the Palomares margin is currently active. The Palomares margin shows a structural pattern comparable to the north Maghrebian margins where Africa-Eurasia plate convergence is accommodated by NE-SW reverse faults, NNW-SSE sinistral faults, and WNW-ESE dextral ones. Contractive structures at this margin contribute to the general inversion of the Western Mediterranean since ~7 Ma, coeval to inversion at the Algerian margin. Shortening at the Alboran ridge and Al-Idrisi faults occurred later, since 5 Ma, indicating a westward propagation of the compressional inversion of the Western Mediterranean.

1. Introduction

Continued NW-SE convergence between the African and European plates is leading to tectonic inversion of Oligocene to Miocene back-arc basins in the western Mediterranean Sea [*Bourgois et al.*, 1992; *Comas et al.*, 1992; *Mauffret et al.*, 1992; *Comas et al.*, 1999; *Billi et al.*, 2011]. Reverse and strike-slip faults related to this tectonic inversion develop in the onshore-offshore margins of these basins (Figure 1) [*Bourgois et al.*, 1992; *Mauffret*, 2007; *Kherroubi et al.*, 2009; *Strzerzynski et al.*, 2010; *Martínez-García et al.*, 2013]. Inversion structures are found along the northern and southern margins of the Algero-Balearic to Alboran basins. Reverse fault systems in the Algerian continental slope, the dextral Yusuf fault, and reverse faulting of the Alboran Ridge, are major active structures related to late Miocene to present-day inversion [*Bourgois et al.*, 1992; *Campos et al.*, 1992; *Deverchere et al.*, 2005; *Domzig et al.*, 2006; *Yelles et al.*, 2009; *Billi et al.*, 2011; *Martínez-García et al.*, 2013; *d'Acremont et al.*, 2014].

The Palomares margin extends from the thinned continental crust intruded by arc magmatism of the Alboran basin in the west to the back-arc oceanic crust of the Algero-Balearic basin in the east (Figure 2) [*Booth-Rea et al.*, 2007]. The margin has been interpreted as formed by large tilted blocks developed during eastward extension [*Mauffret et al.*, 1992] or by transpressive strike-slip structures related to the currently active sinistral fault systems mapped on land (e.g., Terreros, Palomares, and Carboneras fault zones in Figure 2) in the eastern Betics [*Soto et al.*, 2000]. However, previous multichannel seismic (MCS) lines ESCI-Alb1 2b–2c showed the lack of a large extensional fault system at the transition between the Alboran and Algero-Balearic basins [*Booth-Rea et al.*, 2007]. Recent GPS geodetic displacement data, focal mechanisms, and fault slickenline inversion data onshore indicate a present-day compressive tectonic regime for the region

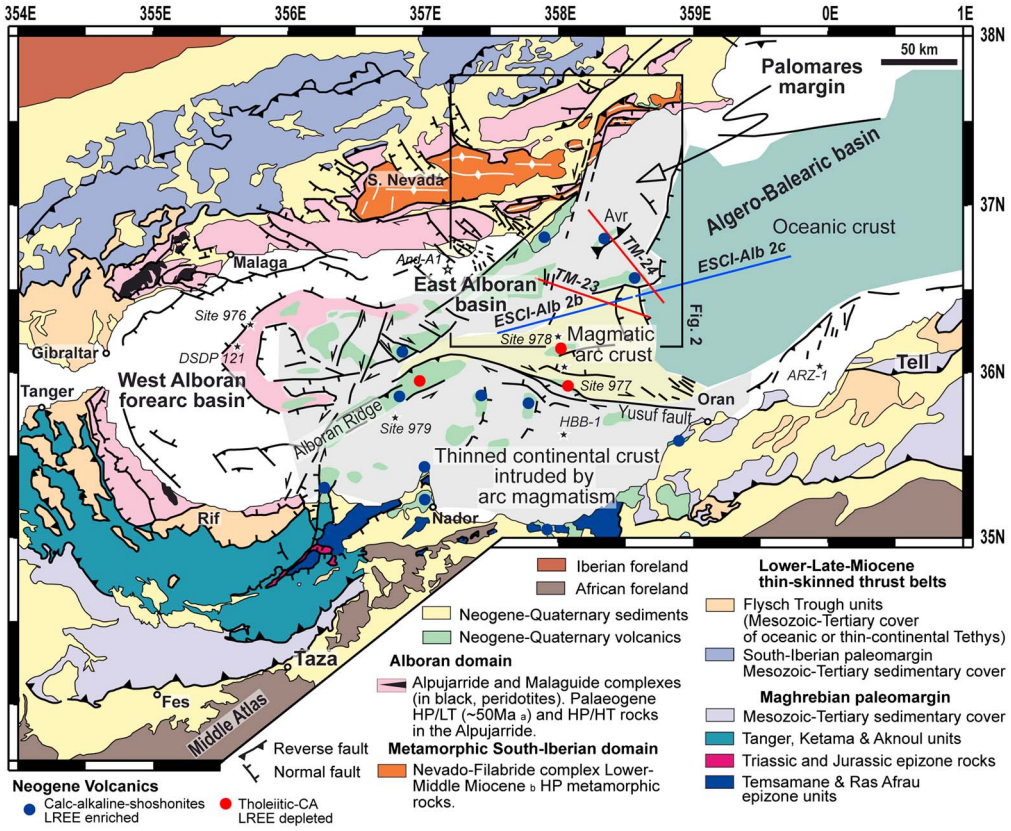

Figure 1. Simplified geological map showing the tectonic domains of the Gibraltar Arc and the Alboran and Algero-Balearic basins [modified from *Comas et al.*, 1999; *Booth-Rea et al.*, 2007; *Martínez-García et al.*, 2013; *d'Acremont et al.*, 2014; *Giaconia et al.*, 2014]. Igneous geochemistry data acquired from *El Bakkali et al.* [1998], *Coulon et al.* [2002], and *Duggen et al.* [2004, 2005]. Age of metamorphism: (a) *Platt et al.* [2005] and (b) *Platt et al.* [2006]. The new seismic profiles presented in this work (TM) are depicted as thick red lines whereas the preexisting seismic profiles (ESCI) are depicted as thick blue lines. Scientific drill sites (DSDP and ODP) and commercial wells in the Alboran Basin are also located.

and for much of the Western Mediterranean (Figure 2) [*Fernández-Ibáñez et al.*, 2007; *Echeverria et al.*, 2013; *Giaconia et al.*, 2013]. The present NW-SE shortening direction (about N140°E) is oblique to the margin and subperpendicular to its individual geological elements that strike N40–50°E, like the Abubacer volcanic ridge (offshore), the Carboneras fault zone (onshore and offshore), and the Sierra Cabrera anticlinorium (onshore, Figure 2).

The debate about the importance of the present-day stress field and the role of active structures in the formation and evolution of the basins of the Western Mediterranean requires the revision of the Palomares margin. For this reason, we collected two new MCS lines across two contrasting areas of the margin. Line TM24 runs across the Abubacer volcanic ridge and is roughly parallel to the present maximum shortening direction (Figure 2). Line TM23 is located in the transition to the East Alboran basin (Figure 1). Simultaneously, we acquired parametric echo sounder subbottom profiles and swath bathymetric data to analyze the most recent sedimentary/tectonic events and relate images of tectonic structures to seafloor relief. The data were acquired on board the Spanish research vessel R/V *Sarmiento de Gamboa* in the frame of the European Science Foundation TopoEurope TOPOMED project [*Gràcia et al.*, 2011] and processed at the Barcelona Center for Subsurface Imaging at CSIC. Furthermore, in order to define the seismostratigraphy and calibrate their age, we performed a correlation between the two new profiles and the published ESCI-Alb 2b and ESCI-Alb 2c profiles that tie the two lines (Figure 2). To study offshore and onshore tectonic regimes and timing of deformation, we correlated the marine seismostratigraphic units with the lithostratigraphic sequence of the Vera and Níjar Neogene basins and compared the tectonic structure interpreted in the seismic images with two onshore geological cross sections across the Sierra Cabrera anticlinorium parallel to the seismic lines. Thus, the main objectives of

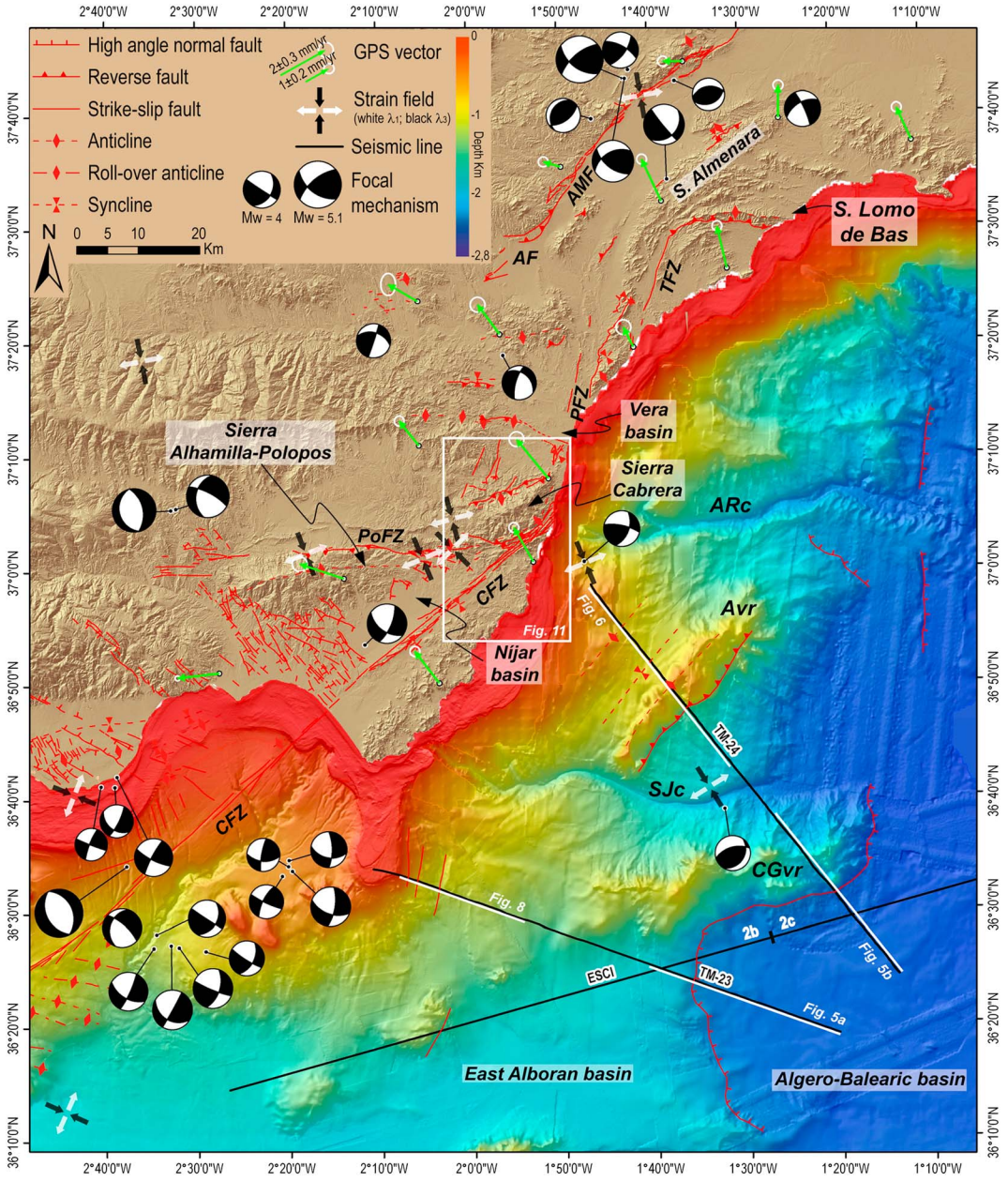

Figure 2. Structural map where the main tectonic structures active during the Quaternary are shown: the Albox fault (AF), the Alhama de Murcia fault (AMF), the Carboneras fault zone (CFZ), the Palomares fault zone (PFZ), the Polopos fault zone (PoFZ), and the Terreros fault zone (TFZ) (see Figure 1 for location) [*Booth-Rea et al.*, 2004a, 2004b; *Masana et al.*, 2004; *Marín-Lechado et al.*, 2005; *Masana et al.*, 2005; *Gràcia et al.*, 2006; *Pedrera et al.*, 2006, 2009; *Sanz de Galdeano et al.*, 2010; *Booth-Rea et al.*, 2012; *Giaconia et al.*, 2012a, 2012b; *Pedrera et al.*, 2012; *Giaconia et al.*, 2013]. Furthermore, focal mechanisms, local stress tensors (from both focal mechanisms and fault slickenline inversion data) [*Stich et al.*, 2003; *Fernández-Ibáñez et al.*, 2007; *Giaconia et al.*, 2013], and GPS geodetic data [*Echeverria et al.*, 2013] are shown. The bathymetric map (100 m grid) of the study area was compiled using digital grids released by SRTM-3, IEO bathymetry [*Ballesteros et al.*, 2008; *Muñoz et al.*, 2008], ICM-CSIC bathymetric dataset [*Gràcia et al.*, 2012], and the MEDIMAP multibeam compilation [*MEDIMAP GROUP et al.*, 2008] at 90 m grid size. The following toponyms are also shown: Alias River canyon (Arc), Abubacer volcanic ridge (Avr), Cresta de los Genoveses volcanic ridge (CGvr), and San José canyon (SJc).

this paper are as follows: (a) to solve the opposite tectonic interpretations of the margin provided by previous authors; (b) to define the origin and timing of the crustal transition at the margin and its following tectonic inversion; and (c) to insert the tectonics of the Palomares margin in the wider context of the late Neogene to present tectonic inversion of the Western Mediterranean.

2. Geological Setting

The western portion of the Algero-Balearic basin together with the East Alboran basin represents the back-arc region of the Gibraltar Arc (Figure 1), an arched orogenic belt formed during the Miocene oblique collision between the Alboran domain and the Iberian and Maghrebian passive margins during westward rollback of a Tethyan slab or delamination in a general context of NW-SE Africa-Iberia convergence[e.g., *Lonergan and White*, 1997; *Zeck*, 1999; *Gutscher et al.*, 2002; *Duggen et al.*, 2003; *Faccenna et al.*, 2004; *Spakman and Wortel*, 2004; *Booth-Rea et al.*, 2007]. The Alboran domain has traditionally been defined as formed by three polymetamorphic terrains, the Malaguide, Alpujárride, and Nevado-Filabride complexes in descending structural order [*Balanyá et al.*, 1997]. Recent work, however, shows that the Nevado-Filabride complex is formed by basement rocks of subducted South Iberian margin [*Booth-Rea et al.*, 2005; *Platt et al.*, 2006]. Thus, following this later interpretation, the Alboran domain should include the Alpujárride and Malaguide complexes, remnants of an earlier orogenic wedge that underwent crustal stacking and high-pressure (HP) metamorphism [*Goffé et al.*, 1989; *Azañón et al.*, 1997; *Booth-Rea et al.*, 2002] associated to Eocene continental collision [*Lonergan*, 1993] dated about 50 Ma [*Platt et al.*, 2005]. In contrast, the Nevado-Filabride complex underwent a later HP metamorphism during the lower to middle Miocene (Figure 2) [*López Sánchez-Vizcaino et al.*, 2001; *Platt et al.*, 2006].

The collision of the Alboran domain with the African and Iberian continental margins occurred during the early to late Miocene after the subduction of the "Flysch Trough" basement formed by oceanic or very thin continental crust (Figure 2) [*Durand-Delga et al.*, 2000; *Luján et al.*, 2006]. Collision and tectonic inversion of both continental margins resulted in a fold-and-thrust belt formed mainly by the detached Mesozoic sedimentary covers of both margins that migrated progressively westward [*Platt et al.*, 1995; *Lujan et al.*, 2003; *Platt et al.*, 2003; *Luján et al.*, 2006]. The Nevado-Filabride complex was exhumed by WSW directed core complex detachments [*Martínez-Martínez et al.*, 2002] during the middle to late Miocene in the hinterland of the collisional system [e.g., *García-Dueñas and Martínez-Martínez*, 1988; *Galindo-Zaldívar et al.*, 1989; *Platt and Vissers*, 1989; *García-Dueñas et al.*, 1992; *Martínez-Martínez and Azañón*, 1997]. The history of formation of the Alboran and Algero-Balearic basins is however much less understood. Between 16 and 8 Ma, the Algero-Balearic basin spread possibly in an E-W direction [*Mauffret et al.*, 2004; *Booth-Rea et al.*, 2007], creating new oceanic-like crust [*Grevemeyer and Ranero*, 2012].

A continued late Miocene to present NW-SE convergence between Africa and Eurasia has produced tectonic inversion of structures in the Betic-Rif internal zones and Alboran and Algero-Balearic basins, and the associated development of several large strike-slip and reverse fault systems [e.g., *Bousquet*, 1979; *Montenat and Ott d'Estevou*, 1990; *Mauffret et al.*, 1992; *Booth-Rea et al.*, 2004a; *Gràcia et al.*, 2006; *Martínez-García et al.*, 2013]. Tectonic inversion at the Algero-Balearic basin along the Algerian margin possibly started at 5–7 Ma and continued during Plio-Quaternary times at N verging thrusts that consist laterally of several fault strands [*Deverchere et al.*, 2005; *Domzig et al.*, 2006; *Mauffret*, 2007; *Kherroubi et al.*, 2009; *Yelles et al.*, 2009; *Strzerzynski et al.*, 2010].

2.1. Tectonics of the Palomares Margin and the Eastern Betics

The Palomares margin is oriented NNE-SSW and bounds the NW end of the Algero-Balearic basin (Figure 1). The continental margin is formed by thinned continental crust intruded by arc volcanism that transits to oceanic crust to the east in a poorly understood manner [*Booth-Rea et al.*, 2007]. Volcanic rocks sampled in basement highs in the East Alboran and Algero-Balearic basins belong to both the tholeiitic and calc-alkaline series (red and blue dots in Figure 1, respectively) with Serravallian to Messinian ages ranging between 12.1–8.7 and 10.1–6.1 Ma, respectively [*Comas et al.*, 1997; *Turner et al.*, 1999; *Duggen et al.*, 2004, 2005]. Tholeiitic series volcanic rocks depleted in light rare earth elements (LREE) characteristic of immature oceanic arcs were sampled in the East Alboran basin (Yusuf and Mansour ridges, red dots in Figure 1) and at the Alboran ridge (Figure 2) [*Duggen et al.*, 2004; *Gill et al.*, 2004]. Furthermore, at the 10–14 km thick crust

domains near the ESCI-Alb lines, LREE-enriched calc-alkaline and shoshonitic rocks have been sampled bearing a continental crust contamination of subduction-related magma [*Hoernle et al.*, 2003; *Duggen et al.*, 2004, 2005]. The westernmost segment of the ESCI-Alb 2b line (Figure 1) has been interpreted as intruded thin continental crust, where arc magmatism could be ≈6 Ma [*Duggen et al.*, 2004], or an embryonic magmatic arc with magmatic accretion coeval to extension [*Booth-Rea et al.*, 2007]. Further east, the ESCI-Alb 2b line (Figure 1) shows a basement seismic structure similar to that of oceanic crust formed at intermediate- to fast-spreading mid-ocean ridges but thicker as expected in a volcanic arc environment [*Ranero et al.*, 1997; *Reston et al.*, 1999; *Booth-Rea et al.*, 2007]. Crustal thickness and structure are similar to oceanic crust in the eastern half of the ESCI-Alb 2c line (Figure 1) [*Booth-Rea et al.*, 2007]. Calibration of the sediments onlapping the basement constrains a minimum age of 10–12 Ma for the oceanic crust and 8–10 Ma in the magmatic arc-influenced region (Figure 2) [*Booth-Rea et al.*, 2007].

Onshore, the central and eastern Betics underwent middle to late Miocene WSW directed extension that attenuated the previous pile of staked metamorphic units of the Alboran domain [*García-Dueñas et al.*, 1992; *Martínez-Martínez and Azañón*, 1997; *Booth-Rea et al.*, 2005, 2007]. This extension was heterogeneous in its style, developing metamorphic core complexes, like the Sierra Nevada elongated dome, and tilted block domains separated by ENE-WSW extensional transfer faults, like the Alpujarras dextral fault that bounds the dome to the south [*Martínez-Martínez et al.*, 2002, 2006a, 2006b].

The boundary between core complex domains onshore and extended regions with magmatic accretion in the East Alboran basin may correspond to extensional transfer faults like the Carboneras sinistral fault [*Rutter et al.*, 2012]. The Carboneras fault zone has been active at least since Serravallian until recent time. The Miocene activity of this fault was essentially strike slip [*Bousquet*, 1979; *Montenat and Ott d'Estevou*, 1990; *Rutter et al.*, 2012]; in contrast, the Plio-Quaternary activity is locally transpressional, as indicated by folding-related unconformities in the latemost Messinian to Pliocene sediments at the Sierra Cabrera [*Bell et al.*, 1997; *Rutter et al.*, 2012] and transpressive structures identified along its offshore segments [*Gràcia et al.*, 2006; *Moreno et al.*, 2008]. The adjacent region onshore and the Palomares margin underwent late Miocene to Quaternary inversion with thrusting, and strike-slip faulting with both dextral and sinistral kinematics [*Montenat and Ott d'Estevou*, 1990; *Comas et al.*, 1999; *Booth-Rea et al.*, 2004a]. The main strike-slip faults in the eastern Betics are sinistral and formed from north to south by the Alhama de Murcia, Terreros, Palomares, and Carboneras faults (Figure 2) [*Montenat and Ott d'Estevou*, 1990; *Booth-Rea et al.*, 2004a; *Masana et al.*, 2004; *Gràcia et al.*, 2006; *Stich et al.*, 2006; *Moreno et al.*, 2008].

3. Methods

3.1. Data Acquisition and Processing

MCS profiles, swath bathymetry, and parametric echo sounder profiles were collected in the Alboran Sea during the TOPOMED-GASSIS cruise Leg 1 carried out in fall 2011 on board the R/V *Sarmiento de Gamboa*. The MCS data were acquired using a 50.15 L (3060 $in.^3$) air gun source array composed by eight G-GUN-II guns deployed at 7.5 m depth. Seismic signal was recorded using a 5100 m long active section Sentinel Sercel SEAL digital streamer with 408 channels (12.5 m channel interval). MCS data were recorded at 2 ms sample rate and 14 s two-way travel time (TWTT) record length. Air gun shots were fired every 50 m, providing a nominal maximum 56 common midpoint (CMP) fold. We processed lines TM23 and TM24 using GLOBE Claritas software (Figures 3a and 3b). Processing steps include crooked streamer geometry implementation, 6.25 m CMP binning, velocity analysis every 100 CMP (625 m), spherical divergence, predictive deconvolution, normal moveout correction, parabolic Radon filter to attenuate multiple energy, stretch muting, inner mute to further attenuate multiple energy in near offsets, and stack. Poststack processing used frequency-wavenumber (*F/K*) to attenuate the remaining coherent noise before a finite difference time migration using a smooth time and space variant velocity model. Finally, the lines were depth converted using velocities extracted from a model of a wide-angle seismic velocity profile coincident with ESCI line 2 [*Leuchters et al.*, 2011]. Depth conversion was done to create a balanced cross-section interpretation of the structure in the seismic lines. Swath bathymetry was acquired with the hull-mounted system ATLAS Hydrosweep DS echo sounder, with frequencies between 14.5 and 16 kHz. The data were processed using CARIS software and integrated with existing data to produce digital terrain

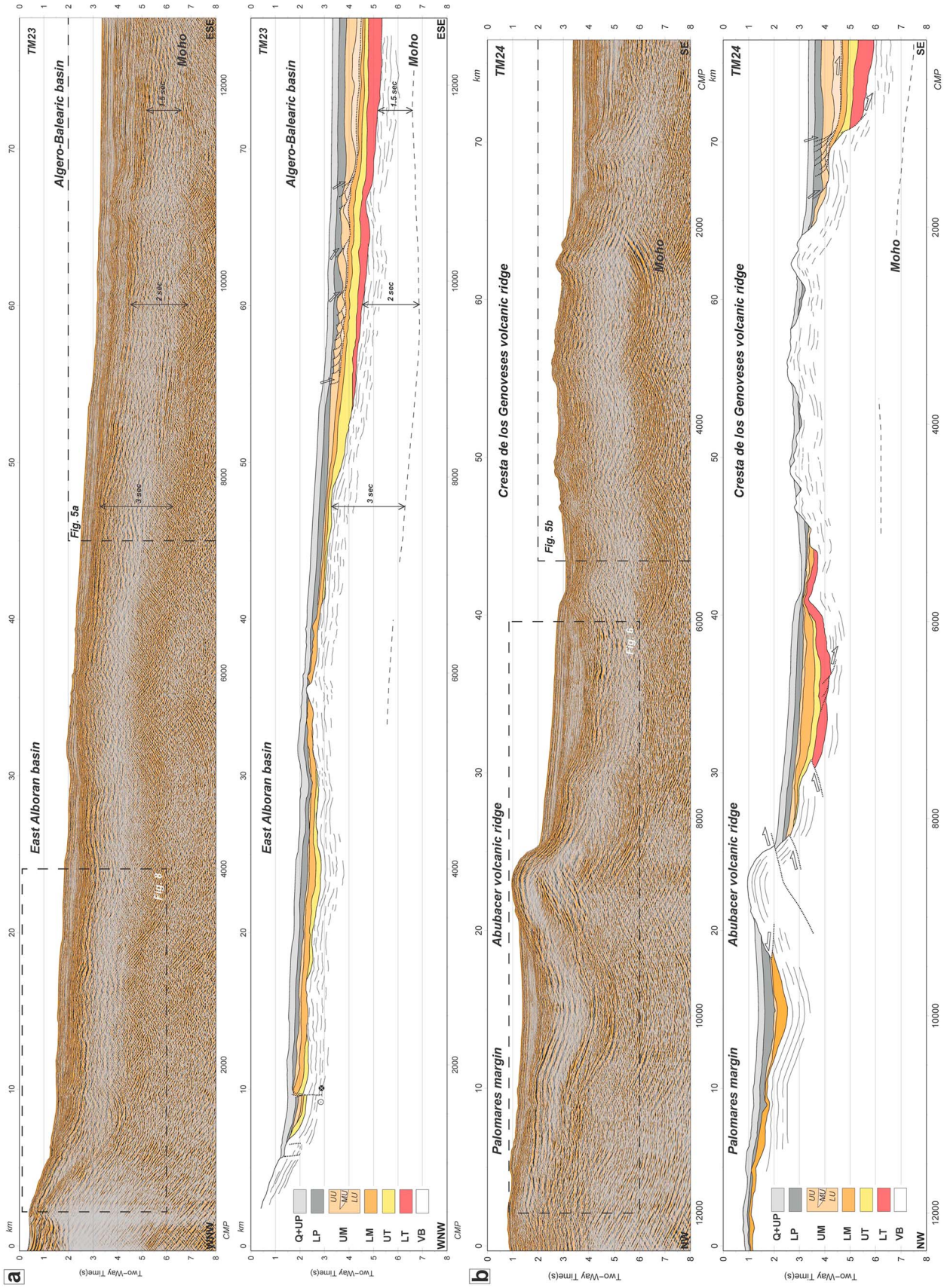

Figure 3. Time migration and line drawing of MCS profiles TM23 (a) and TM24 (b), with the location of the main features (see Figure 1 for the line locations). Rectangles correspond to zooms of the seismic profiles presented in Figures 5a, 5b, 6, and 8. The lithoseismic units recognized in the MCS line are Plio-Quaternary units (Q + UP, Quaternary-upper Pliocene; LP, lower Pliocene), Messinian units (UM, upper Messinian; MU, mobile subunit; LM, lower Messinian), upper Tortonian unit (UT), lower Tortonian unit (LT), and finally the volcanic basement (VB).

models of 50 m grid size. High-resolution narrow-beam parametric echo sounder subbottom profiles were acquired using the ATLAS Parasound P.35. This system uses a primary frequency of 18–20 kHz, and a secondary frequency of 1.5–4 kHz. During the TOPOMED-GASSIS cruise, a continuous-wave single pulse was used, with frequencies of 4 kHz. The pulse length was 0.50 ms, and the pulse interval was 300 ms, with a maximum vertical resolution of 0.6 ms. These data show detailed geological information of the uppermost few tens of meters below the seafloor.

3.2. Balanced Cross Section

The structural analysis to calculate the detachment depth of the fault propagation fold recognized in the TM24 line was carried out by applying the excess area graphical technique proposed by *Epard and Groshong* [1993].This method predicts the detachment depth of a fault propagation fold plotting a set of geological horizons in an excess area versus depth diagram. The depth coordinates of this diagram are obtained by an arbitrary horizontal reference, while the excess area coordinates are obtained by calculating the area comprised between the folded geological horizon and the horizontal line that joins points of the geological horizons considered as undeformed/unfolded. This set of coordinates defines a straight line with a slope that is the fault displacement; meanwhile, its intersection with the depth axis is the depth to the detachment with respect to the arbitrary horizontal reference.

4. Results

A major outcome obtained from the MCS lines and parametric subbottom profiles is the characterization of shortening and transpressional structures in the Palomares margin. Furthermore, the MCS lines provide important information about the crustal structure of the Algero-Balearic basin at the Palomares margin.

4.1. Seismic Stratigraphy of the Margin

To define the main seismostratigraphic discordances and units of the margin, we used the seismostratigraphic sequence described by *Jurado and Comas* [1992] for the northern Alboran basin and by *Medaouri et al.* [2014] for the southern Alboran and Algero-Balearic basins. In detail, we used the Ocean Drilling Program (ODP) sites 977 and 978 for the ages of Plio-Quaternary seismostratigraphic units [*Comas et al.*, 1999; *Booth-Rea et al.*, 2007] and the Andalucia-A1 [*Jurado and Comas*, 1992], Habibas-1 Sonatrach commercial well, and Arzew-1 Sonatrach core drill (ARZ-1) [*Medaouri et al.*, 2014] for the late Miocene sequence (Figure 1). In addition, we correlated the late Miocene units with stratigraphic sequence exposed onshore at the Vera and Níjar basins, which is well defined and dated, thus improving the onshore-offshore correlation provided by *Booth-Rea et al.* [2007] for the ESCI-Alb seismic lines that tie lines TM23 and TM24 (Figure 4).

The onshore-offshore correlation for the late Miocene units presented in this paper is based on the fact that the study region of the Palomares margin, and the Vera and Níjar basins were not semienclosed marginal (or peripheral) basins as the Sorbas-Tabernas basin, but open basins connected with the Mediterranean Sea even during the Pliocene, except for a short time interval in the Messinian during the Salinity Crisis [*Riding et al.*, 1998; *Braga et al.*, 2003; *Fortuin and Krijgsman*, 2003]. This is confirmed by open marine/pelagic marls of the Chozas Fm. [*Hsü et al.*, 1973, 1977], Abad Mb. [*Sierro et al.*, 2001; *Fortuin and Krijgsman*, 2003], and Cuevas Fm. [*Mather*, 1993; *Stokes and Mather*, 2000], which globally shows ages between the late Tortonian and the Pliocene (~8.5–3.3 Ma). The onshore-offshore correlation for the Messinian Salinity Crisis (MSC) units is speculative and under debate. However, the widely accepted model for the MSC proposed a two-step development [*Clauzon et al.*, 1996; *Briand*, 2008; *CIESM*, 2008], and the synchronous onset and development of the Primary Lower Gypsum (PLG) or Lower Evaporites (LE) deposits in the Mediterranean Sea [*Lugli et al.*, 2010] are elements that allow us to propose an onshore-offshore stratigraphic correlation for the Palomares margin and the Níjar-Vera basins. During the first MSC stage (5.97–5.60 Ma) [*Gautier et al.*, 1994; *Krijgsman et al.*, 1999; *CIESM*, 2008; *Manzi et al.*, 2013], primary shallow-water evaporites (PLG/LE) accumulated in semienclosed marginal or peripheral basins that are currently exposed onshore the eastern Betics (Yesares Fm. 5.96–5.67 Ma) [*Martín and Braga*, 1994; *Riding et al.*, 1998; *Krijgsman et al.*, 2001]. At this stage, the evaporitic MSC facies had not deposited in the deep sectors of the Alboran and Algero-Balearic basins, but the euxinic shales and dolostones [*CIESM*, 2008; *Manzi et al.*, 2013]. During the second MCS stage (5.60–5.55 Ma) [*Gautier et al.*, 1994; *Krijgsman et al.*, 1999; *CIESM*, 2008; *Manzi et al.*, 2013], a substantial fall in sea level of the Mediterranean accounts for the deposition of thick MSC halite mobile unit in the deep basins

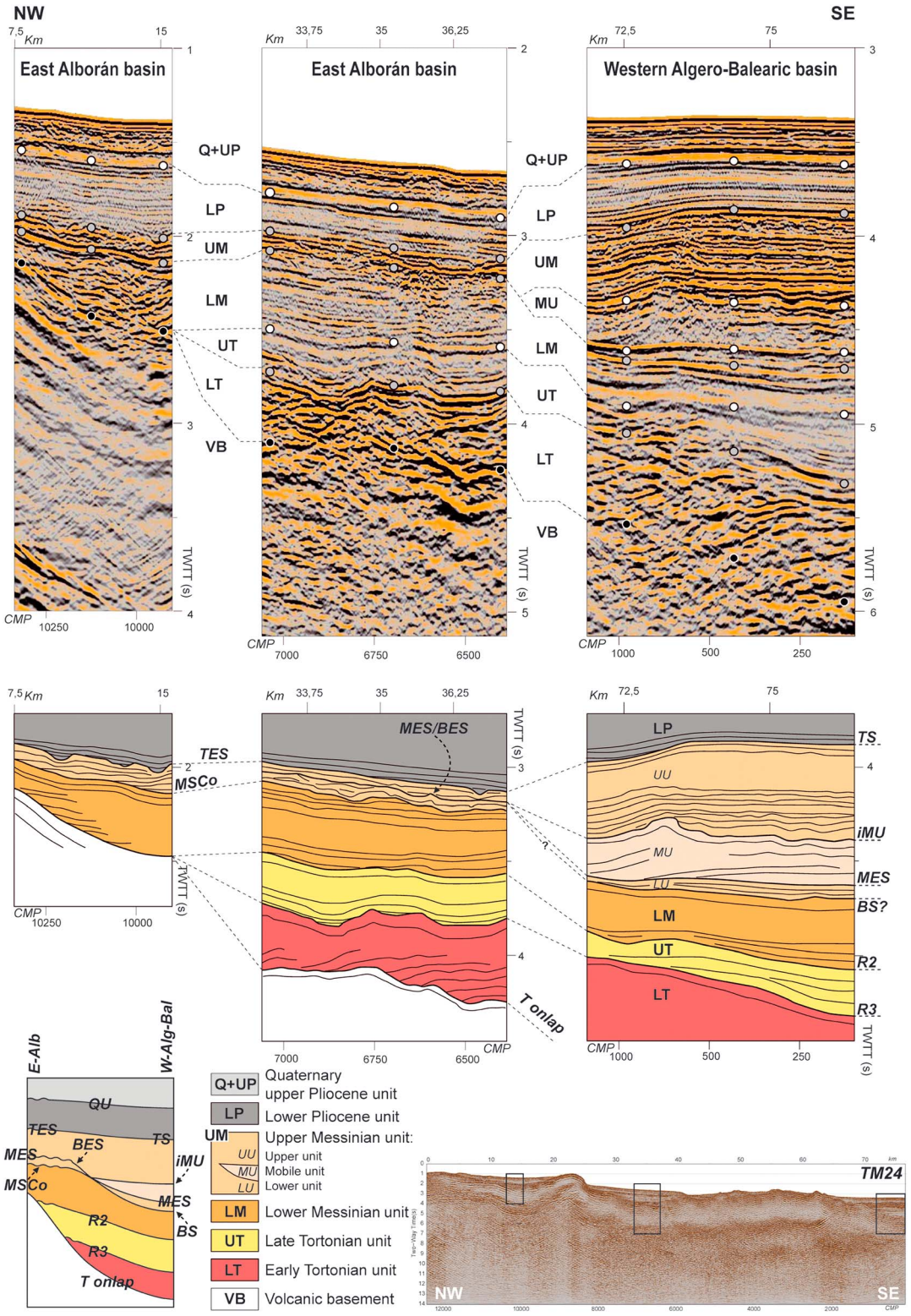

Figure 4. Synthetic stratigraphic column of the late Neogene sediments of the Níjar-Vera basins correlated with the lithoseismic units identified on lines TM24 and TM23, following the seismostratigraphic correlation proposed by *Booth-Rea et al.* [2007]. The following geologic surfaces were recognized in the MCS lines: the Quaternary Unconformity (QU), the Pliocene Unconformity (TES/TE), the Intra-Messinian Unconformity (iMU), the Messinian Erosional Surfaces (MES), the Messinian Salinity Crisis Onset Unconformity (MSCo), the Base Erosion Surface (BES/BS), and the Tortonian Unconformities (R2 and R3). The lithoseismic units recognized in the MCS lines are Plio-Quaternary units (Q + UP, Quaternary-upper Pliocene; LP, lower Pliocene), Messinian units (UM, upper Messinian including UU, upper subunit, MU, mobile subunit, and LU, lower subunit; LM, lower Messinian), upper Tortonian unit UT, lower Tortonian unit LT, and finally the volcanic basement, VB.

while the slope marginal areas were undergoing an intense and polygenic erosion producing the Messinian Erosion Surface (MES) [*Lofi et al.*, 2005, 2011] as in the Níjar and Vera basins affecting the Yesares Fm. top [*Fortuin and Krijgsman*, 2003; *Omodeo Salé et al.*, 2012]. Finally, the reflooding Lago Mare event occurred (5.55–5.33 Ma) [*CIESM*, 2008; *Manzi et al.*, 2013], starting first in the deep basins (5.55–5.42 Ma) and later in the marginal basins (5.42–5.33 Ma). The age of the Feos Fm. between 5.67 and 5.3 Ma shows that the Lago Mare reflooding in the Vera and Níjar basins occurred at the same time as in the deep basins (5.67–5.54 and 5.3 Ma) [*Fortuin and Krijgsman*, 2003; *Aguirre and Sánchez-Almazo*, 2004]. However, the Lago Mare event has been recently interpreted to reach Zanclean ages in the more marginal Sorbas basin (Zorreras Mb.) [*Do Couto et al.*, 2014b; *Clauzon et al.*, 2015].

The main bounding seismic surfaces are described below from top to bottom (Figures 3 and 4).

Quaternary Unconformity (QU): In the westernmost part of both MCS lines, this surface is an erosional truncation onlapped by the overlying upper Pliocene to Quaternary unit Q + UP, up to km 30 of line TM23 and km 10 of line TM24 (Figures 3a and 3b). Eastward into the basin, this surface evolves to a paraconformity defined mostly by one reflection, except at the end of line TM23 where it evolves into an angular unconformity, starting from km 55 of the line (Figure 3a). The age of this surface has been inferred from the underlying upper Pliocene unit UP that is probably equivalent to the Pliocene Cuevas marls deposited onshore at the Níjar and Vera basins between 5.3 and 3.2 Ma [*Aguirre*, 1998].

Pliocene Unconformity (Top Erosion Surface (TES)/Top Surface (TS)): This surface is an erosional truncation that coincides with the top of the Messinian or the base of the Zanclean that is onlapped by the transgressive lower Pliocene unit LP (Figure 4) along most of the MCS lines (up to km 32.5 of line TM23 and km 45 of line TM24, Figures 3a and 3b), but it evolves to an angular unconformity or a paraconformity basinward to the east at the Algero-Balearic basin (Figures 3 and 4). This unconformity coincides with the one described by *Driussi et al.* [2014] in the Balearic Promontory as the Top Erosion Surface (TES), at the proximal region, and the Top Surface (TS), in the deep basin that bounds the Upper Unit (UU) of the MSC record at the top.

Intra-Messinian Unconformity (iMU): This surface occurs in both MCS lines but only to the east at the Algero-Balearic basin (starting from km 55 of line TM23 and km 67.5 of line TM24, Figures 3a and 3b) where it starts as an angular unconformity onlapped by the upper Messinian unit UM, and farther to the east, it evolves to a paraconformity (Figure 4).

Messinian Erosional Surface (MES): This surface was described all over the Mediterranean Sea [e.g., *Lofi et al.*, 2005, 2011] and the Alboran Sea (M or R1 reflector) [*Ryan and Hsü*, 1973; *Jurado and Comas*, 1992; *Riding et al.*, 1998; *Comas et al.*, 1999] as an erosional truncation affecting the Messinian PLG or LE deposits [*Lugli et al.*, 2010]. This surface occurs locally as an erosive surface (e.g., between km 25 and 40 of line TM24 of Figure 3b and middle column of Figure 4), but it evolves to an angular unconformity or a paraconformity basinward to the east at the Algero-Balearic basin (from km 55 of line TM23 and km 70 of line TM24, Figures 3a and 3b and right column of Figure 4). In this region, it is imaged as a high-amplitude reflection with negative polarity indicating a decrease in seismic velocity from the overlying Messinian salt mobile unit MU to the underlying marly lower Messinian unit LM. This unconformity has been described by *Driussi et al.* [2014] in the Balearic Promontory as the Base Erosion Surface (BES), at the proximal region, and the Base Surface (BS) in the deep basin that bounds the Lower Unit (LU) of the MSC record at the bottom.

Messinian Salinity Crisis Onset Unconformity (MSCo): This surface is an angular unconformity along most of the MCS lines onlapped by the upper Messinian unit UM (Figures 3 and 4). Locally, this surface seems erosive on the underlying lower Messinian unit LM (between km 25 and 40 of line TM24, Figure 3b, and middle column of Figure 4). To the east of both MCS lines (from km 55 of line TM23 and km 70 of line TM24, Figures 3a and 3b), this surface seems to merge with the high-amplitude reflection with negative polarity of the MES-R1. This unconformity has been described all over the Mediterranean Sea both onshore and offshore [e.g., *CIESM*, 2008; *Manzi et al.*, 2013].

Tortonian Unconformities 1 and 2 (R2 and R3): These surfaces are erosional truncations [Jurado and Comas, 1992] that occur to the west of both MCS lines onlapped by the lower Messinian unit LM and the upper Tortonian unit UT, respectively (Figures 3 and 4). Both unconformities evolve to angular unconformities and paraconformities basinward to the east at the Algero-Balearic basin.

The main seismostratigraphic units are described below from top to bottom (Figures 3 and 4). To calculate unit thickness, we used RMS velocities picked during MCS processing for normal moveout correction.

Unit Q + UP: The upper Pliocene to Quaternary unit is bounded at the bottom by the QU or locally by the high-amplitude reflective upper Messinian unit UM below. This unit defines mostly a paraconformity in both MCS lines but locally appears erosive in the western part of line TM24 onlapping and infilling troughs and channels. Unit Q + UP has a continuous high-frequency reflectivity and a maximum thickness of ~0.3 s TWTT (≈230 m assuming a 1.55 km/s velocity) with good lateral continuity (Figures 3 and 4). By correlation with ODP site 978, unit Q + UP is formed by clay with sandstone and some pebbly interbedding containing abundant bioclasts deposited between the late Pliocene and the present, corresponding to subunit Ia [*Jurado and Comas*, 1992; *Comas et al.*, 1999]. This unit should be equivalent to the late Pliocene and Quaternary continental and shallow marine sediments of the Molata Fm. and the deltaic and fluvial conglomerates of the Gochar Fm. onshore at the Níjar and Vera basins [*Booth-Rea et al.*, 2007] according to the biostratigraphic ages (3.1–0 Ma) obtained from planktonic and foraminifera analysis on the Habibas well (SE Alboran basin) by *Medaouri et al.* [2014].

Unit LP: The lower Pliocene unit is bounded by the QU at the top and the TES/TS at the bottom although locally it overlies the lower Messinian unit LM. To the west at the Alboran Basin unit LP onlaps the upper Messinian unit UM infilling possible fluvial erosion channels (e.g., western part of line TM24) and rests paraconformable to the east at the Algero-Balearic basin in both MCS lines (Figures 3 and 4). This unit reaches a maximum thickness of ~0.4 s TWTT (≈400 m assuming a 2.05 km/s velocity) and is characterized mostly by low-reflectivity facies typically bounded by two more reflective lithoseismic units (Figures 3 and 4). Unit LP offshore includes middle Pliocene clays and silty clays cored in ODP sites 977 and 978 corresponding to subunit Ib [*Jurado and Comas*, 1992; *Comas et al.*, 1999] and is probably equivalent to the Pliocene marls of the Cuevas Fm. deposited onshore at the Níjar and Vera basins between 5.3 and 3.2 Ma [*Aguirre*, 1998; *Booth-Rea et al.*, 2007]. This unit corresponds mostly to the EP unit proposed by *Medaouri et al.* [2014] that is formed by sand turbidities and mud mounded carbonate ramp at the Algero-Balearic basin and by sands and sandy marls levels and lithothamnion calcareum at the southern Alboran basin, both with ages between 5.42 and 3.1 Ma.

Unit UM: The upper Messinian unit is bounded by the TES/TS, at the top, and MSCo or BS, at the bottom (Figures 3 and 4). The unit UM shows high-amplitude reflections compared with the bounding units in both the Alboran and Algero-Balearic basins (Figure 4). This unit appears erosive, onlapping the lower Messinian unit LM at the Alboran basin; meanwhile, it defines an angular unconformity at the Algero-Balearic basin (Figures 3 and 4). In the Alboran basin, unit UM includes the MSC units exposed onshore at the Níjar and Vera basins that are (from bottom to top) the Yesares Fm. deposited after 5.96 Ma (equivalent to "Lower Evaporites" of Sicily, the Gessoso-Solfifera Formation of the Northern Apennines) [*Krijgsman et al.*, 2001; *Fortuin and Krijgsman*, 2003] and Feos Fm. deposited between 5.67–5.54 and 5.3 Ma (Lago Mare facies equivalent to "Upper Evaporites" of Sicily, the Colombacci Formation of the Northern Apennines) [Fortuin and Krijgsman, 2003]. In the Algero-Balearic basin, the UM unit reaches a maximum thickness of ~0.75 TWTT composed by ~0.5 TWTT of the nonhalite UM (≈600 m assuming a 2.4 km/s velocity) and ~0.25 TWTT of MU (Figures 3 and 4). In this region, according to *Driussi et al.* [2014] and *Medaouri et al.* [2014], the unit UM is composed (from top to bottom) by three subunits: the upper subunit (UU), the Messinian salt mobile subunit (MU), and the lower subunit (LU) (Figures 3 and 4).

The *subunit UU* shows high-amplitude reflections compared with the bounding units being limited by the TS at the top and the iMU at the base (Figures 3 and 4). This subunit is equivalent to the unit UU of *Medaouri et al.* [2014] that has been cored at the ALG-1 and ARZ-1 wells where it includes marls and brittle anhydrites probably corresponding to the Lago Mare facies marls of Feos Fm. onshore.

The *subunit MU* occurs only at the eastern ends of the MCS lines in the Algero-Balearic basin where it appears as a transparent seismic unit overlying a high-amplitude reflection with negative polarity (MES) that indicates a decrease in seismic velocity in the underlying sedimentary unit, typical of Messinian salts (Figures 3 and 4). This unit reaches a maximum thickness of ~0.25 TWTT (≈500 m assuming a 4.2 km/s velocity, Figures 3a and 3b) and is bounded by the MES at the base and the iMU at the top. This subunit is equivalent to the unit MU of *Medaouri et al.* [2014] cored at the ALG-1 and ARZ-1 wells and formed by halite and dirty salt that probably deposited during the erosion of the Yesares Fm. onshore between 5.60 and 5.55 Ma [*Gautier et al.*, 1994; *Krijgsman et al.*, 1999; *Manzi et al.*, 2013].

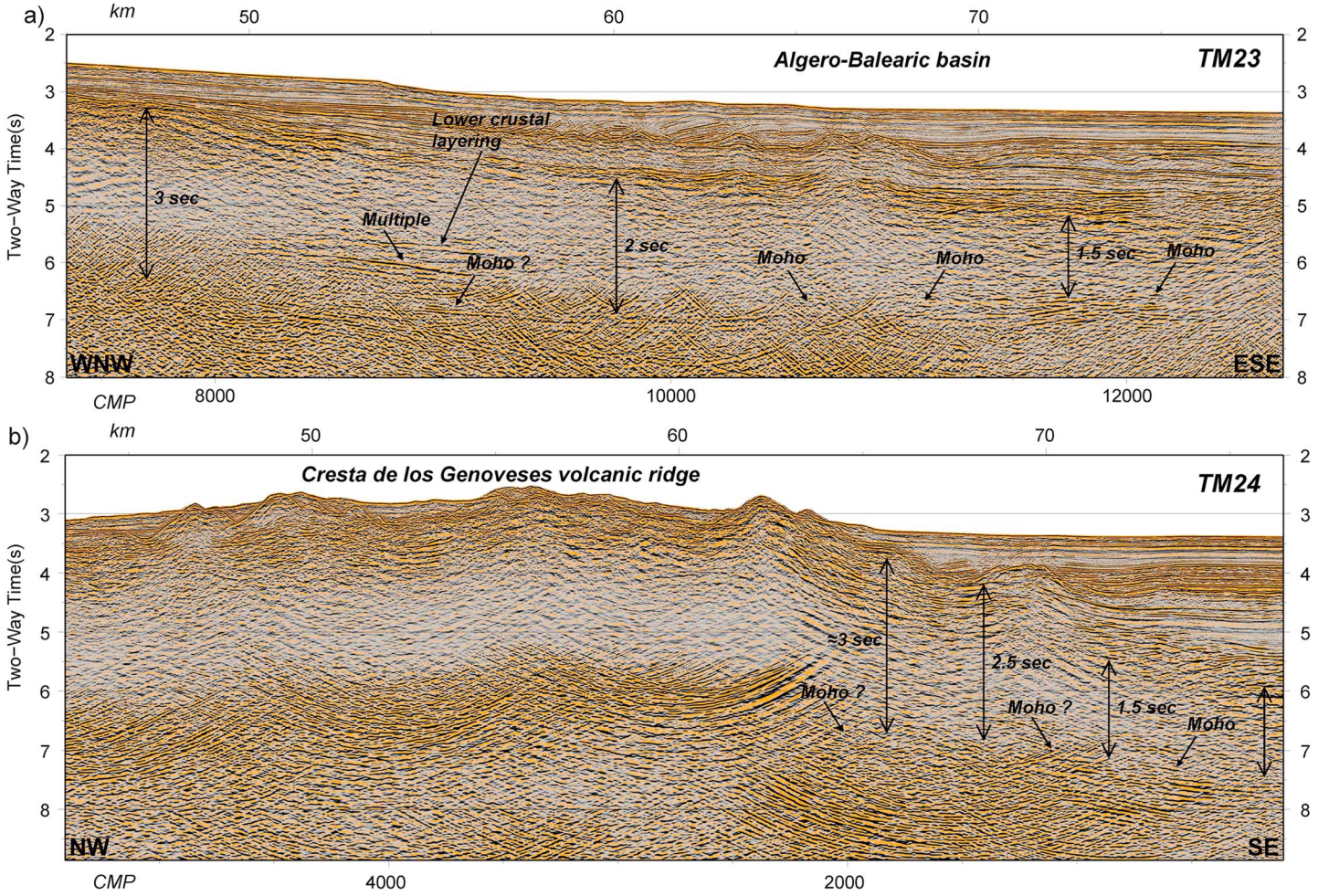

Figure 5. Blow-ups of the time migration of (a) TM23 and (b) TM24 showing the Moho reflections (see Figures 3a and 3b for their location).

The *subunit LU* underlies the high-amplitude reflection, with negative polarity appearing as a transparent seismic unit compared with this unconformity and the underlying unit (unit LM). This subunit is bounded by the MES at the top and by another unconformity at the base, corresponding most probably to the BS (right column of Figure 4) that defines the base of unit UM in this deep-basin region. This subunit is equivalent to the unit LU of *Medaouri et al.* [2014] formed by plastic gray marls and gypsum cored at the ALG-1 and ARZ-1 wells.

Unit LM: The lower Messinian unit is bounded by unconformities MSCo at the top and R2 at the bottom in the Alboran basin (except to the west where it onlaps the basement); meanwhile, at the Algero-Balearic basin, locally, it is bounded by the BS at the top. This unit is characterized by discontinuous low-amplitude reflections in the eastern and central parts of the MCS lines showing a decrease in seismic reflectivity compared to the overlying unit UM or the MU (Figures 3 and 4). The seismic facies of this unit indicates low-velocity and low-reflectivity sediments corresponding to hemipelagic marl and shale that have been cored at the southern Alboran and Algero-Balearic basins with biostratigraphic ages of 6.96–5.73 and 7.24–5.96 Ma, respectively (subunit LU) [*Medaouri et al.*, 2014]. Toward the west, especially in line TM24, unit LM shows different seismic facies characterized by higher reflectivity, probably indicating an increase in siliciclastic content toward the shore. Furthermore, along TM24 (between km 10 and 15), this unit onlaps the volcanic basement infilling a syncline and showing discontinuous high-amplitude reflections that indicate the syntectonic deposition during fault propagation folding of the Neogene Abubacer volcanic ridge (Figures 3b and 5). Unit LM reaches a maximum thickness of ~0.5 s TWTT (≈700 m assuming a 2.9 km/s velocity) and probably is equivalent to the upper members of the Turre Fm. onshore in the Níjar and Vera basins, which includes the

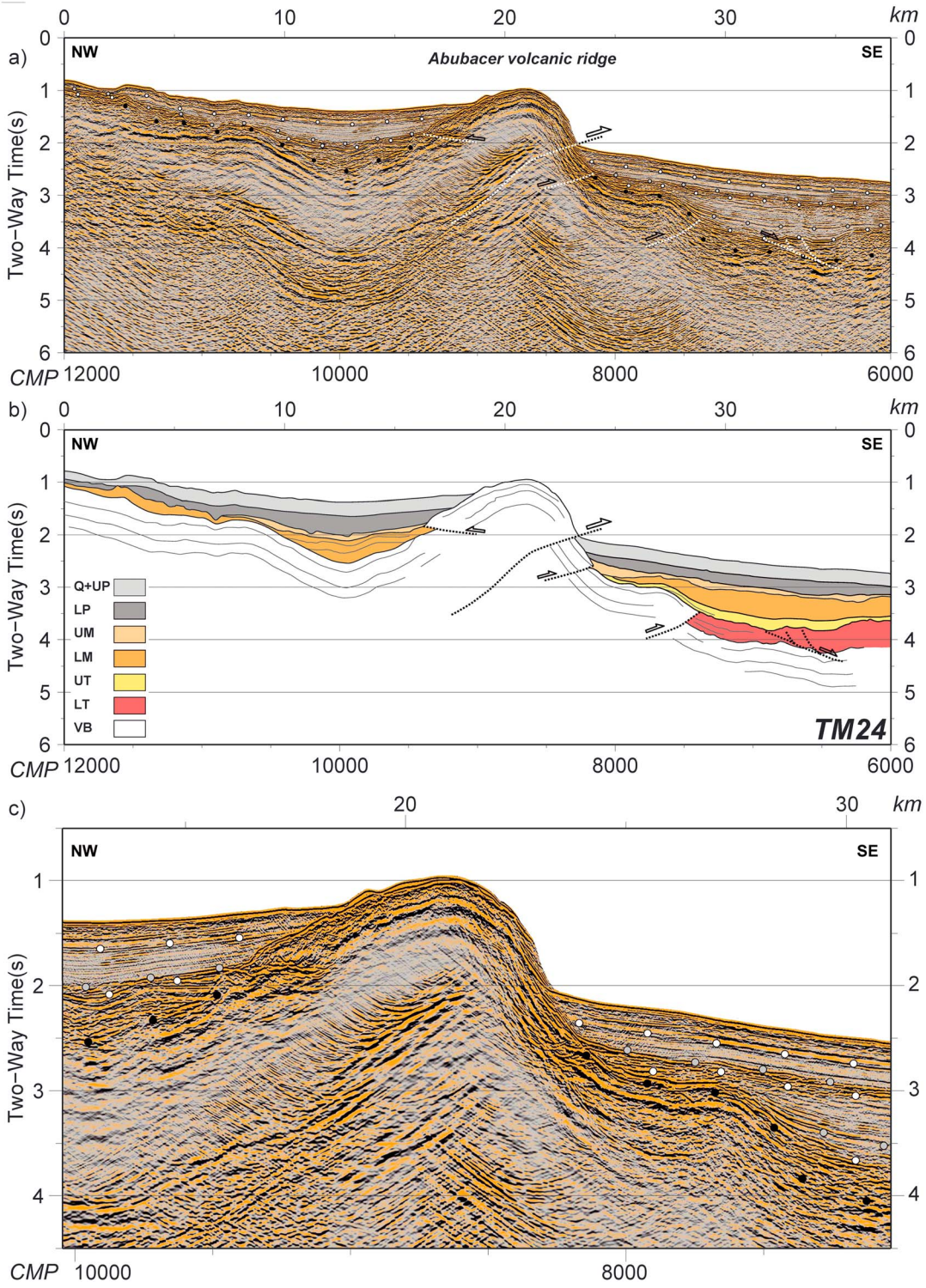

Figure 6. (a) Blow-up of the time migration of TM24 seismic profile and (b) line drawing interpretation (see Figure 3b for the blow-up location). (c) Blow-ups of Figure 6a showing the main thrusts forming the Abubacer fault system. The main features and lithoseismic units are named as in Figure 3a. Notice the thrusts and associated fault propagation fold affecting the volcanic basement.

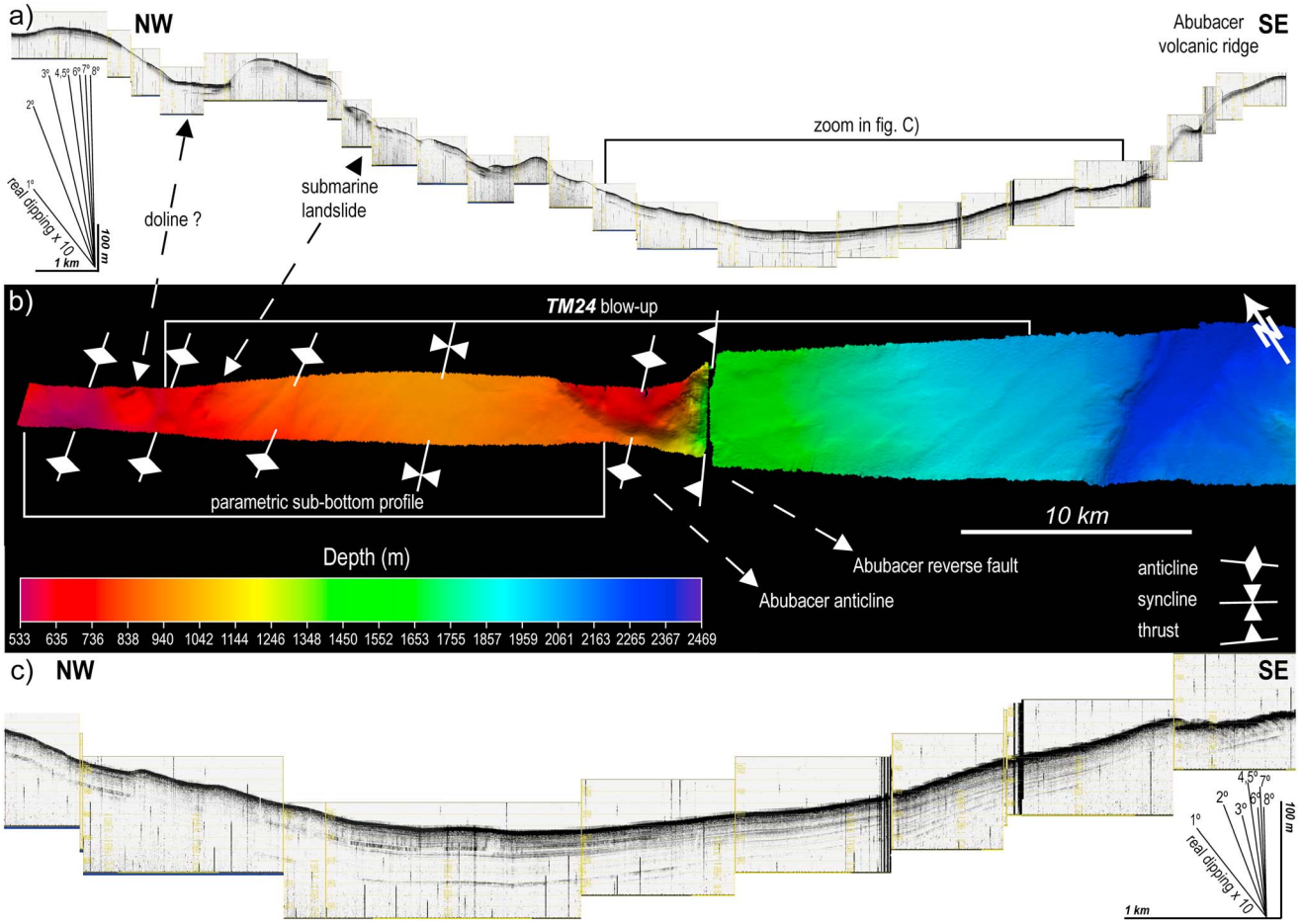

Figure 7. (a) Parametric subbottom profile along seismic line TM24 that shows anticlines and synclines affecting the Quaternary sediments. (b) Bathymetric data indicate a N40°E strike for the anticlines and synclines, detected both in the basement and in the Plio-Quaternary sedimentary cover. (c) Blow-up of the open hanging wall syncline of the Abubacer thrust in Figure 7a where the upper Plio-Quaternary sediments (unit Q + UP) show fold-onlapping growth strata toward the hinge.

Abad marls deposited before the Messinian Salinity Crisis (~7.4–5.96 Ma) [*Krijgsman et al.*, 2001] and its marginal equivalent, the Cantera Mb. (7.24–5.96 Ma) [*Völk*, 1966; *Sierro et al.*, 2001]. The Messinian units UM and LM together correspond to the Unit II defined from well data by *Jurado and Comas* [1992], which includes evaporites, carbonate, volcanic, and volcaniclastic levels interbedded with fine-grained sediments.

Unit UT: The upper Tortonian unit is bounded by unconformities R2 at the top and R3 at the bottom onlapping unit LT below in the Alboran basin but laying paraconformable on it in the Algero-Balearic basin (Figure 4). This unit is characterized by low-amplitude facies reaching a maximum thickness of ~0.25 s TWTT (≈350 m assuming a 2.9 km/s velocity) in the central part of line TM24 (Figures 3b and 4), and it is absent in the western part of the lines. The seismic facies of this unit is consistent with the lithologies cored at the northern Alboran basin (clays to pebbly sandstones of Unit III) [*Jurado and Comas*, 1992], the southern Alboran basin (shales and marls with sand intervals and pyroclastic level of Unit T with ages between 6.96 and 9.26 Ma) [*Medaouri et al.*, 2014], and the southern Algero-Balearic basin (gray marls with sands and pyroclastic intervals of Unit T with ages between 7.24 and 9.26 Ma) [*Medaouri et al.*, 2014]. This unit probably corresponds to hemipelagic fine-grained sediments exposed onshore at the Níjar and Vera basins like the "Lower" Abad member [*Sierro et al.*, 2001; *Fortuin and Krijgsman*, 2003], its marginal equivalent Azagador Member (8–7.24 Ma) [*Völk*, 1966; *Martín et al.*, 2003], and the late Tortonian Chozas Fm. marls and silts [*Ruegg*, 1964; *Völk and Rondeel*, 1964; *Völk*, 1966].

Unit LT: The lower Tortonian unit is bounded by the R3 at the top and is characterized by discontinuous high-amplitude reflections that onlap the volcanic basement toward the east of the MCS lines reaching a maximum thickness of ~0.5 s TWTT (≈700 m assuming a 2.9 km/s velocity, Figures 3 and 4). This unit corresponds to Unit IV defined by *Jurado and Comas* [1992] cored at the northern Alboran basin including clays and silty

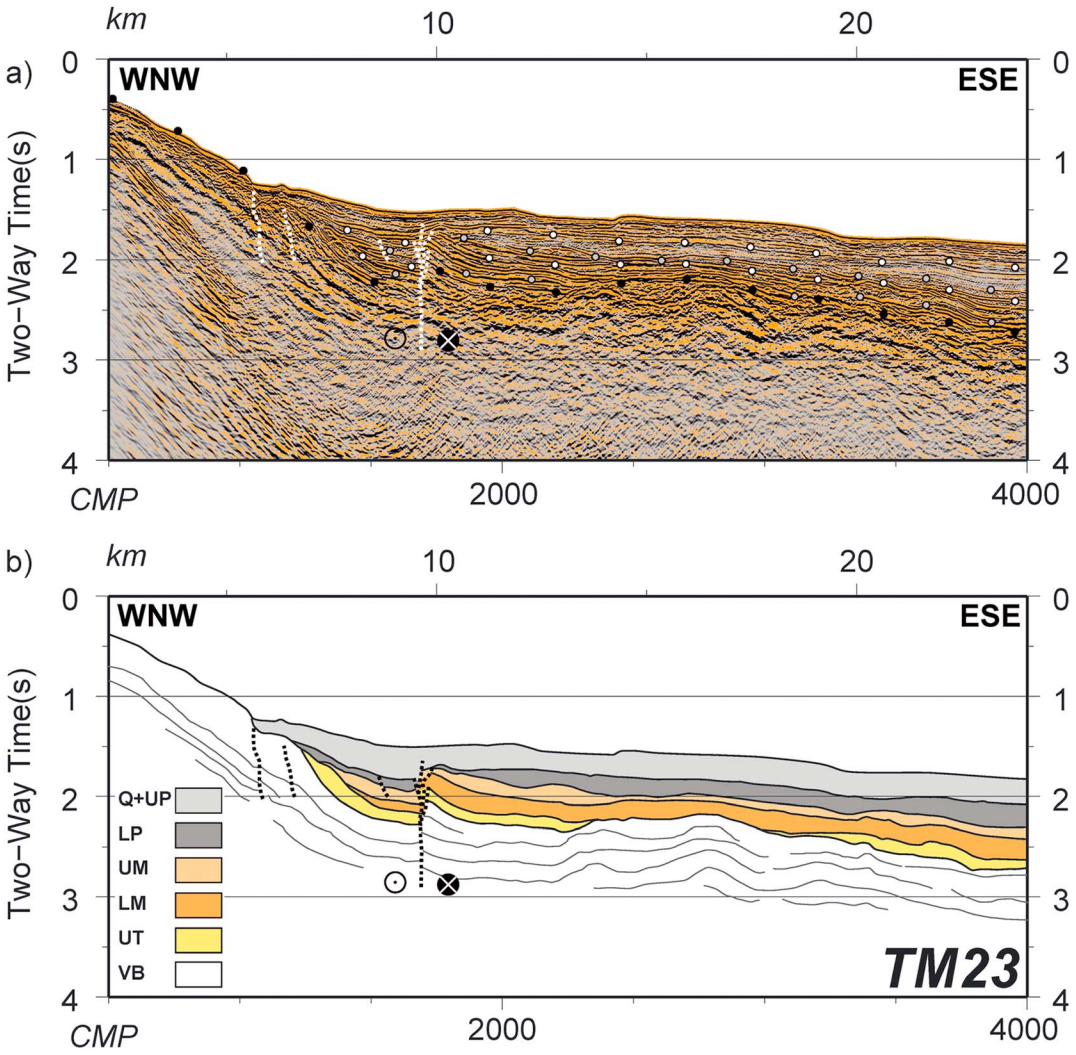

Figure 8. (a) Blow-up of the time migration of line TM23 and (b) line drawing interpretation (see Figure 3a for the blow-up location). The lithoseismic units recognized in the MCS line are named as in Figure 3a.

clays with sandy interbeds. At the southern Alboran and Algero-Balearic basins, it is made up of clays and slits with sandy and marl intervals with biostratigraphic ages between 9.26 and 11.7 Ma (Unit S) [*Medaouri et al.*, 2014]. Nevertheless, the seismic facies of this unit at the Palomares margin is not consistent with these lithologies but with coarser and harder lithologies as the Tortonian volcanosedimentary breccias (Brèche rouge) or early Tortonian mixed carbonate-siliciclastics that crop out onshore at Cabo de Gata, south of the Níjar basin [*Montenat and Ott d'Estevou*, 1990; *Martín et al.*, 2003].

4.2. Crustal-Type Transition at the Palomares Margin

The basement imaged by both TM23 and TM24 MCS lines is characterized by a bright top reflection and high-amplitude continuous reflections at its uppermost part that progressively fade away at depth (Figures 3a, 3b, and 5). Eastward, the top of the basement is more reflective, with low-continuity and comparatively smaller amplitude reflections at the Cresta de los Genoveses (east of line TM24, Figures 3b and 5b), where a thin Plio-Quaternary sedimentary cover (unit Q + UP) overlies a dome-like structure formed by subalkaline basalts [*Duggen et al.*, 2008]. This dome-like structure may represent an area of magmatic accretion formed by intrusions and arc volcanism. Calc-alkaline and shoshonitic volcanic rocks and granodiorites with a continental crust contamination component have been dredged at the Eastern Alboran basin and the nearby Abubacer volcanic ridge [*Duggen et al.*, 2008],

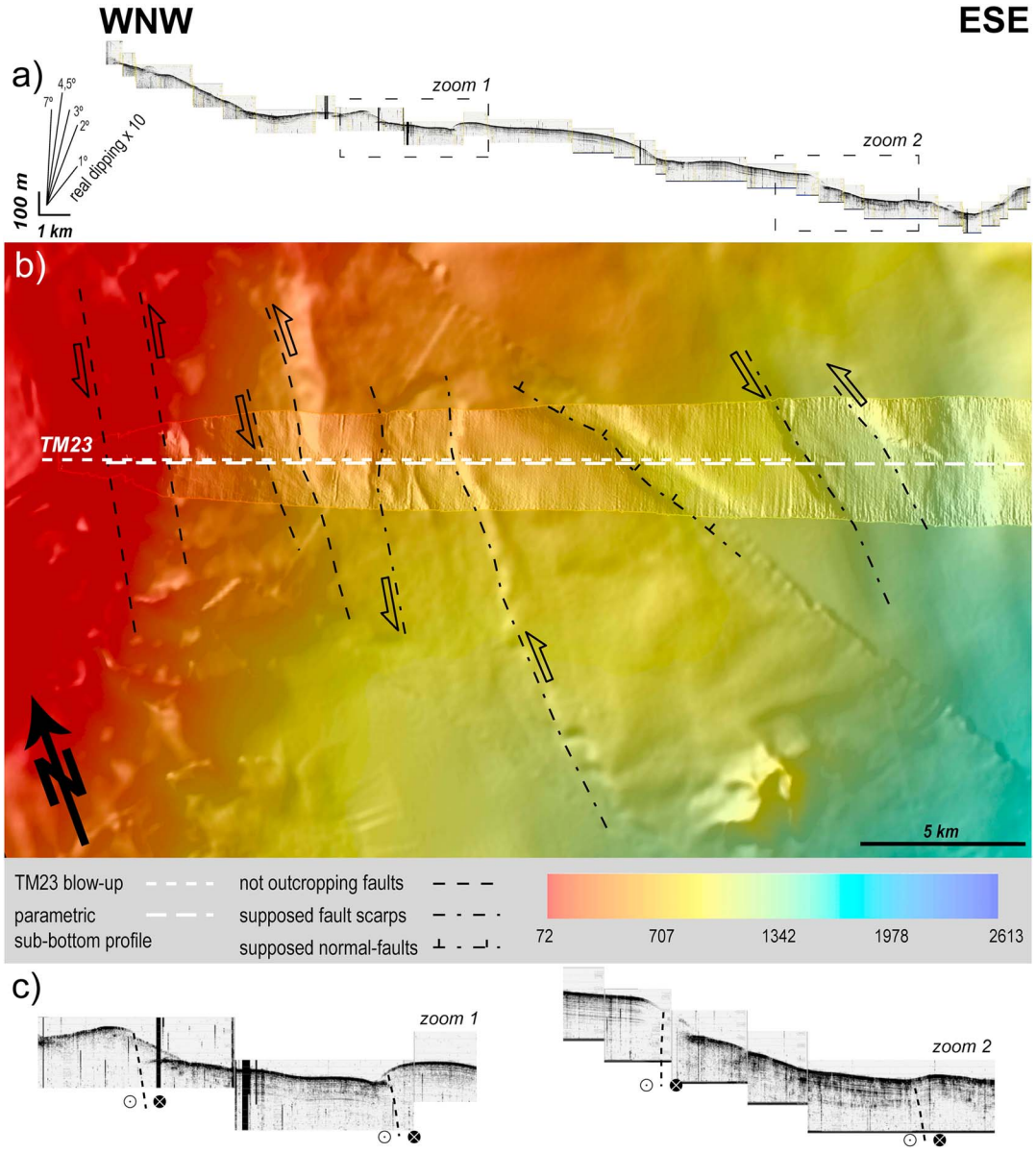

Figure 9. (a) Parametric subbottom profile along seismic line TM23 that shows subvertical scarps corresponding to submarine slides or faults with both reverse and normal displacement affecting the Quaternary sediments. (b) Bathymetric data indicate that the scarps have a N10–20°E strike. Faults (drawn with dotted line) at the western part of the line correspond to the vertical faults imaged by line TM23. (c) Blow-up of the scarps imaged by the parametric subbottom profile. Because of the lack of useful kinematic constraints, the sinistral kinematic of faults (imaged in both the MCS line and the parametric subbottom profile) is deduced from their strike to be congruent with those of the Palomares fault system (N10–20°E).

indicating that the basement here is formed by thinned continental crust strongly intruded by subduction arc-related magma.

The Moho reflections are imaged in both TM23 and TM24 lines, mainly at the east, at a depth between 5.5 and 7.5 s TWTT (Figure 5). The basement above the Moho reflections thins toward the east, especially in line TM23 where it decreases along 25 km distance from 3 to 1.5 s TWTT (or ~9 to ~4–5 km assuming a 6 km/s velocity, Figure 5a). Furthermore, the transition from a ~9 km thick heavily intruded or arc-type crust to a 4–5 km thick more typical oceanic crust at the Palomares margin occurs without fault block structures (Figure 5). This crustal transition has been interpreted to occur by eastward increasing thinning of the continental crust

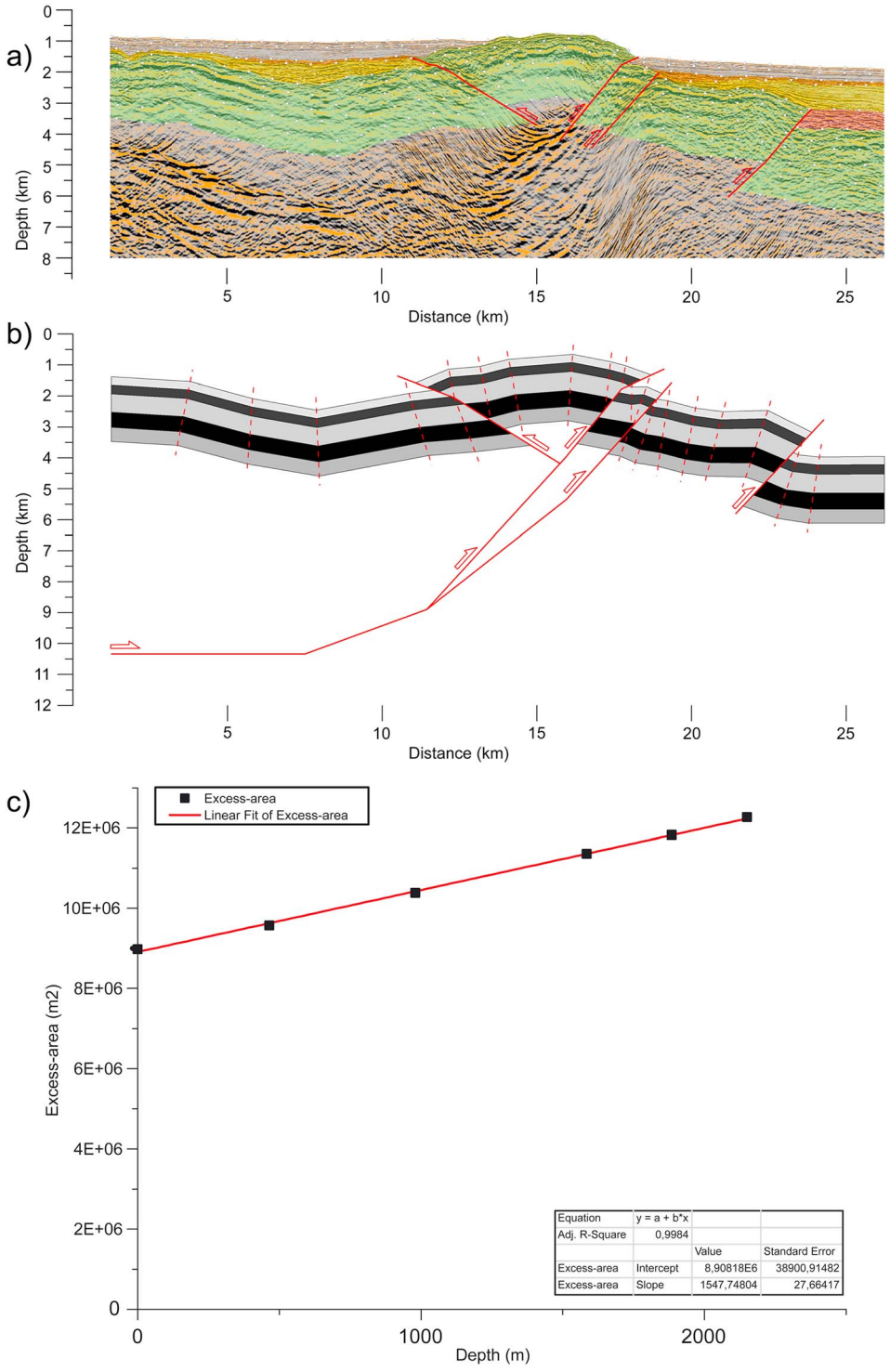

Figure 10. (a) Depth converted blow-up of MCS profile TM24 with the following lithoseismic units (from top to bottom): Quaternary-upper Pliocene unit Q + UP(light gray), lower Pliocene unit LP (dark gray), upper Messinian unit UM (orange), lower Messinian unit LM (yellow), upper Tortonian unit UT (red), and volcanic basement (green). (b) Balanced cross section from MCS profile TM24 for the prekinematic volcanic basement. The depth of the basal detachment of the fault propagation fold was calculated with the excess area graphical technique proposed by *Epard and Groshong* [1993]. (c) Excess area versus depth diagram plotting six geological horizons from the balanced cross section of the prekinematic volcanic basement of seismic profile TM24 (Figures 10a and 10b). The geological horizons define a linear equation ($y = a + b \cdot x$) that indicates a fault displacement of the entire fault system (except the southeastern thrust) of about 1.5 km (b = the line slope, with an error of ±27.66 m) and a depth to the detachment of about 10 km (a = depth intercept of the line, with an error of ±128.04 m).

that has been pervasively intruded by arc magmatism because of the opening of the Algero-Balearic basin during Serravallian to Messinian time [*Mauffret et al.*, 2004].

4.3. Shallow Crustal Structures

The Abubacer ridge is the surface expression of a fault propagation fold that deforms the sediment cover and igneous basement of the Palomares margin (line TM24, Figure 6). The main thrust, referred to as Abubacer fault, has a SE-ward sense of displacement, folding and uplifting the northwestern hanging wall fault block. Minor thrusts occur on the limbs of the Abubacer anticline that are sealed by the lower Pliocene unit LP, including a back thrust to the west with NW directed displacement (Figure 6). Westward, between the Abubacer anticline and the coastline, a syncline is filled by uppermost Tortonian to lower Messinian syntectonic sediments of unit LM (Figure 6). Upper Messinian and lower Pliocene sediments (units UM and LP) infilling the syncline show growth strata toward the fold hinge (Figure 6). The footwall of the Abubacer fault contains a syncline filled by lower Messinian syntectonic sediments (unit LM, Figures 4 and 6). Another minor SE displacing thrust and associated fault propagation fold deform the northwestern limb of this syncline, displacing the Neogene volcanic basement onto the lower Tortonian unit LT. This structure is sealed by the upper Tortonian unit UT (Figure 6).

The parametric subbottom profile along line TM24 (Figure 7) images anticlines and synclines deforming Quaternary sediments that are visible in the MCS line. Anticlines occur both near the coast to the NW (between CMP 11500 and 10500 in Figure 6) and at the Abubacer ridge (at CMP 9000 of Figure 6), at either side of the main syncline (Figure 7). The Plio-Quaternary sediments (subunits Ia + b) infilling the hanging wall syncline of the Abubacer thrust show fold-onlapping growth strata toward the hinge (Figure 7). Bathymetric data along TM24 line indicate a N40°E strike for the anticlines and synclines and a length of about 30 km for the Abubacer fault. Reverse faulting and folding associated with the Abubacer fault produced the ~700 m high structural relief of the Abubacer ridge where the volcanic basement crops out at the seafloor (Figures 6 and 7). The integration of MCS reflection lines, parametric subbottom profiles, and bathymetric data shows a good congruence between structural and morphological features, especially at the Abubacer ridge region where the main syncline corresponds to a bathymetric depression, and the Abubacer ridge is formed by an anticline, as well as other minor anticlines. The main submarine canyons dissecting the Palomares margin, related to the San José and Alias rivers, flow subparallel to the synclines and cut transverse to the Abubacer anticline. This geometry suggests that the fold-and-thrust system growth and the dissection processes were coeval, resulting in submarine canyon deflections (Figure 2).

Line TM23 shows a positive strike-slip flower structure affecting from the volcanic basement to the entire sediment cover (Figure 8). The southeastern fault block is uplifted and folded, defining a transpressive strike-slip structure affecting a Plio-Quaternary depocenter. Plio-Quaternary sediments appear syntectonic because they are folded and show growth geometry (units Q + UP and LP, Figure 8) controlled by the transpressive structure. The upper Tortonian unit UT represents the youngest prekinematic unit with respect to the strike-slip faults (Figure 8).

Parametric subbottom images along line TM23 together with the bathymetry show subvertical scarps that correspond either to mass movement scars or to faults with reverse and normal displacement that affect Quaternary sediments and the seafloor (Figure 9). These scarps strike N10–20°E parallel to the Palomares fault system and may represent the offshore extension of the fault system south of the Sierra Cabrera anticlinorium (Figure 2).

4.4. Geometry of the Abubacer Fault and Related Structures

The depth conversion of seismic line TM24 (Figure 10a) was carried out using a velocity model based on velocities obtained from wide-angle velocity modeling of a profile coincident with ESCI-Alb 2 line [*Leuchters et al.*, 2011]. The depth conversion was carried out only for the Abubacer region to provide a realistic geometry and dimensions (both depth and fault plane/strata dipping angles) of the main fault propagation fold. Globally, the main thrust and the minor ones are of relatively low angle, dipping 20–40° and displacing the basement up to 1 km (Figure 10a).

The depth section allows construction of a balanced cross section of the fault propagation fold (Figure 10b). We applied the excess area graphical technique proposed by *Epard and Groshong* [1993] to obtain the depth of the main detachment (see section 3.2). Using the balanced cross section, we have plotted a set of six

geological horizons of the volcanic basement defining layers with constant thickness and affected by the fault propagation fold in an excess area versus depth diagram (Figure 10c). The six points define a linear equation ($y = a + b \cdot x$) in the diagram that indicates a fault displacement of the entire fault system (without considering the southeastern thrust because of the lack of any arbitrary horizontal reference that intercepts equivalent displaced layers) of about 1.5 km and a detachment depth at 10 km that is close to the brittle-ductile transition (details of the brittle-ductile transition are provided in the supporting information). Furthermore, the balanced cross section allows calculation of a shortening of ~3 km and a vertical displacement of ~2 km produced by the Abubacer fault system.

5. Discussion

5.1. Synthesis of the Structures Observed at the Palomares Margin

The western Algero-Balearic basin opened in an E-W direction by the development of oceanic-like crust [*Pesquer et al.*, 2008] between 16 and 8 Ma [*Mauffret et al.*, 2004; *Booth-Rea et al.*, 2007]. This age interval is mostly coeval to the age (between 12 and 6 Ma) of arc-type rocks that intruded the thinned continental crust of the East Alboran basin and that crop out at Cabo de Gata, onshore the Palomares margin [*Comas et al.*, 1997; *Turner et al.*, 1999; *Duggen et al.*, 2004, 2005]. The crustal transition from thinned intruded continental crust (e.g., at Cabo de Gata, onshore, and at the Cresta de los Genoveses, offshore) to oceanic crust eastward occurs progressively, without a fault block structure at the Palomares margin like at typical rifted margins [e.g., *Ranero and Perez-Gussinye*, 2010]. These data together with the age of volcanic rocks in the region suggest that much of the extension from Serravallian to latemost Tortonian was accommodated by magmatic accretion, with extensional tectonics being comparatively minor, although, at the Palomares region, there is no evidence of a pure magmatic arc crust between the intruded continental crust and the oceanic one as documented in the ESCI-Alb 2 line to the south [*Booth-Rea et al.*, 2007].

Shortening structures at the Palomares margin indicate that early contraction probably started in latemost Tortonian to Messinian (~8–7 Ma), inferred from the syntectonic deposit of unit LM on the back limb of the Abubacer fault propagation fold (Figure 6). The main bathymetric highs of the margin appear related to these shortening structures that have uplifted and folded the igneous basement of the margin. The fold geometry affects the bathymetry as indicated by the highs and depressions of the Abubacer volcanic ridge (Figure 2). Furthermore, plutonic granodiorites have been exhumed in the core of the Abubacer anticlinal ridge, proving the nonvolcanic origin of this bathymetric high. Thus, the relief of the margin is strongly influenced by the late Miocene shortening structures rather than by tilted middle-late Miocene extensional fault blocks, as suggested by *Mauffret et al.* [1992]. These shortening structures are presently active since they fold Plio-Quaternary sediments that locally show growth strata and produce pronounced seafloor relief that deflects submarine canyons (e.g., Alias River and San José submarine canyons) (Figure 2). A M_w 3.8 earthquake (30 June 2005, Instituto Geográfico Nacional, http://www.ign.es) produced a thrust focal mechanism at 11 ± 0.3 km depth, about 50 km away from the coast (Figure 2) [*Fernández-Ibáñez et al.*, 2007], that supports active shortening. The focal depth of this earthquake is similar to the detachment depth of the Abubacer fault. Considering that the Abubacer fault system initiated its activity in latemost Tortonian or early Messinian (~8–7 Ma), the obtained slip rate of the system is about 0.2 mm/yr, with a vertical slip rate of about 0.25 mm/yr (at the Abubacer volcanic ridge) and a horizontal shortening of about 0.4 mm/yr. As expected, the vertical slip rate is higher than that at the Carboneras fault zone (0.05–0.1 mm/yr) [*Bell et al.*, 1997].

Timing of transpressive strike-slip structures imaged on line TM23 is considerably younger than deformation at the Abubacer volcanic ridge, probably starting in the Pliocene and controlling Plio-Quaternary sedimentation. Sinistral focal mechanisms in the region and faulted and folded Plio-Quaternary sediments indicate that transpressive faulting and related folding are currently active and may indicate that the Palomares fault system continues southward offshore (Figure 2) [*Stich et al.*, 2006; *Fernández-Ibáñez et al.*, 2007].

5.2. Integration of Onshore-Offshore Structural Data

Shortening structures at the Palomares margin are coeval to the tectonic inversion at the eastern Betics in the Tabernas-Sorbas, Vera [e.g., *Bousquet*, 1979; *Weijermars et al.*, 1985; *Sanz de Galdeano and Vera*, 1992; *Stapel et al.*, 1996; *Booth-Rea et al.*, 2004a; *Giaconia et al.*, 2013; *Do Couto et al.*, 2014a], and Huércal-Overa basins

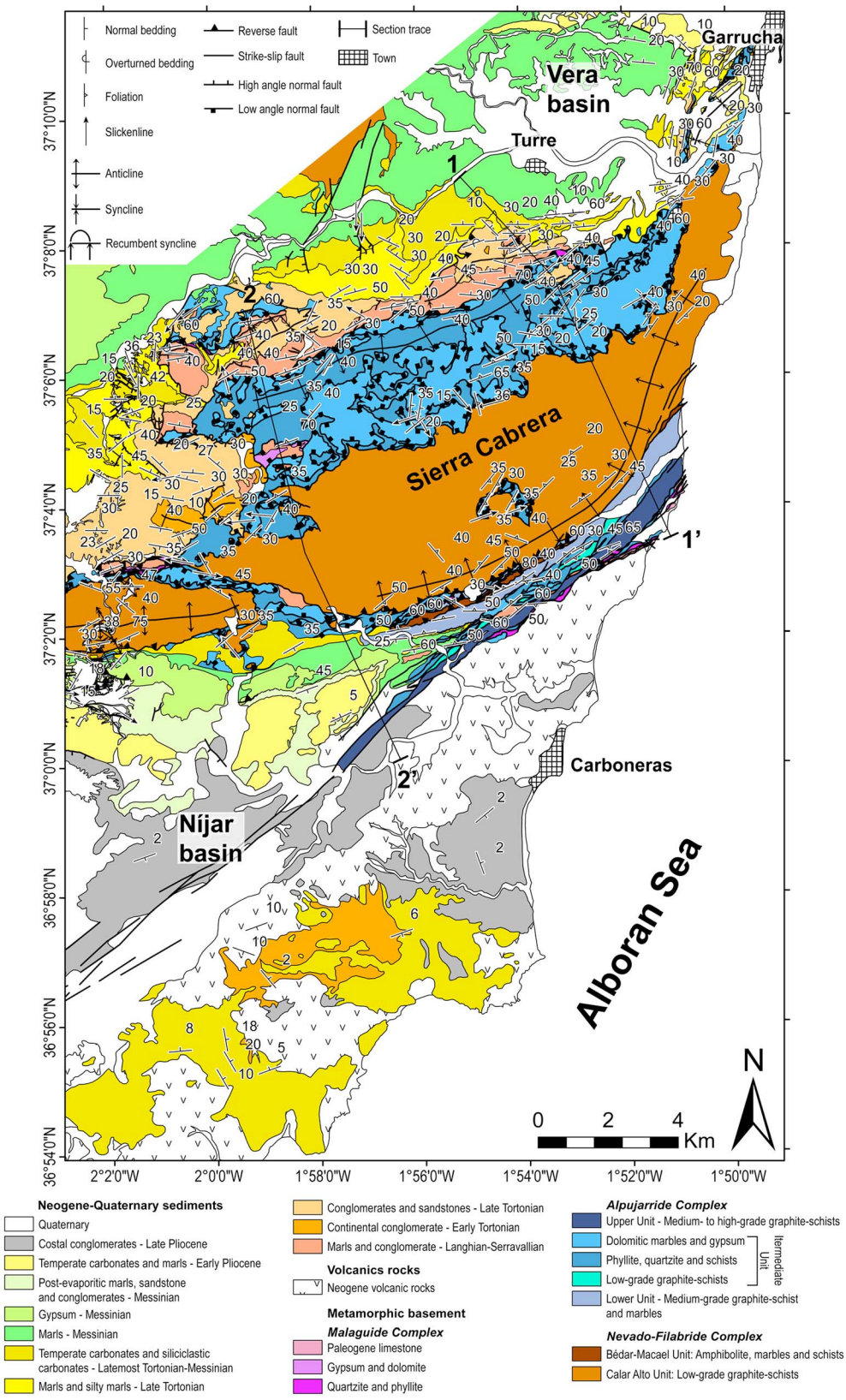

Figure 11. Geological map of the Sierra Cabrera anticlinorium and surrounding Neogene sedimentary basins (located in Figure 2): the Vera and the Níjar basins, to the north and to the south, respectively. Furthermore, two cross sections subparallel to seismic line TM24 and to the main shortening direction in the region are located (Figure 12).

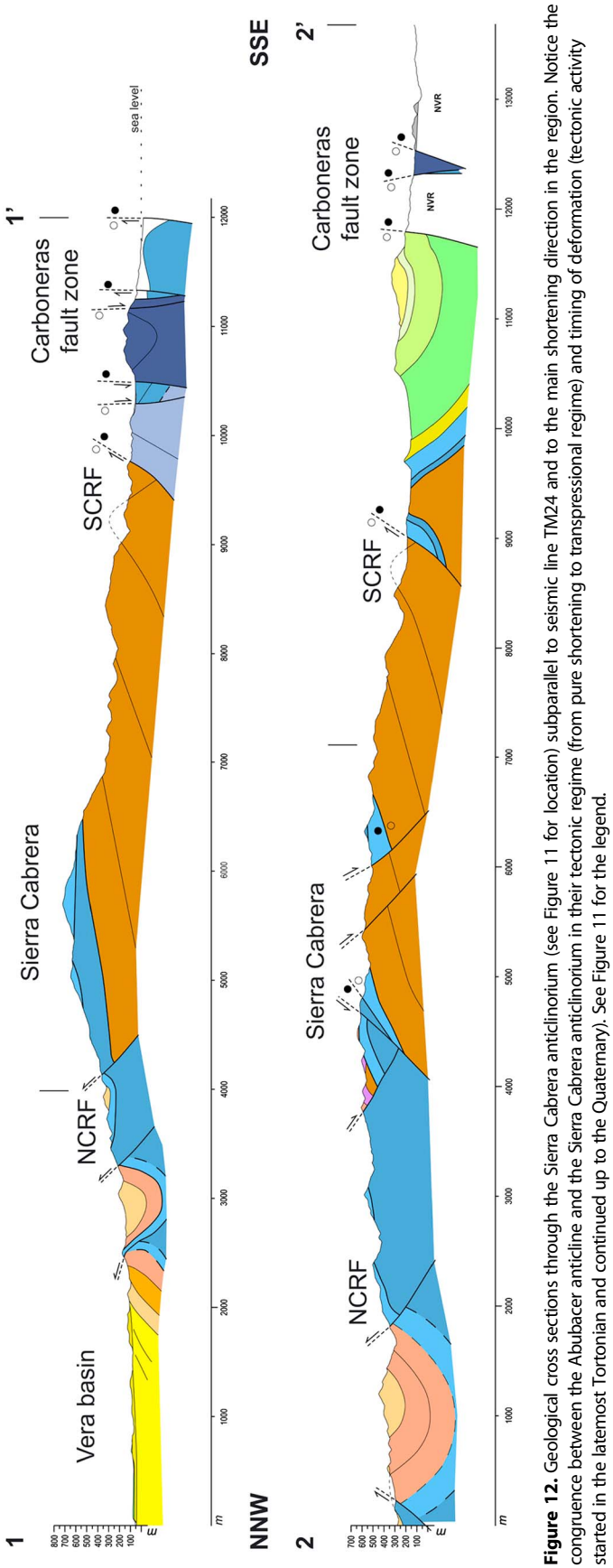

Figure 12. Geological cross sections through the Sierra Cabrera anticlinorium (see Figure 11 for location) subparallel to seismic line TM24 and to the main shortening direction in the region. Notice the congruence between the Abubacer anticline and the Sierra Cabrera anticlinorium in their tectonic regime (from pure shortening to transpressional regime) and timing of deformation (tectonic activity started in the latemost Tortonian and continued up to the Quaternary). See Figure 11 for the legend.

[e.g., *Mora*, 1993; *Garćia-Meléndez et al.*, 2003; *Augier*, 2004; *Meijninger*, 2006; *Pedrera et al.*, 2010]. To compare deformation on land and offshore, we have mapped the Sierra Cabrera anticlinorium. Similar to the Abubacer anticline, the Sierra Cabrera anticlinorium strikes N50–60°E, that is, normal to the present-day shortening stress field, and is bounded by north and south dipping reverse faults that define a pop-up structure (Figures 11 and 12). These structures affect the metamorphic and volcanic basement and cut Tortonian to early Pliocene sediments (Figures 11 and 12). The initial growth of the Sierra Cabrera anticlinorium is documented by progressive unconformities in the latemost Tortonian Azagador member to the north, corresponding to the base of unit LM [*Booth-Rea et al.*, 2007], and by unconformities in the latemost Messinian to Pliocene sediments to the south [*Rutter et al.*, 2012]. Furthermore, the Quaternary activity of the North and South Cabrera reverse faults is indicated by geomorphic analysis that related a set of geomorphic features (e.g., rectilinear mountain fronts, highly dissected and V-shaped valleys, and positive *SLk* anomalies) to their tectonic activity [*Giaconia et al.*, 2012a]. The Sierra Cabrera pop-up anticlinorium and sinistral Palomares and Terreros fault systems in the eastern Betics are structures similar to those mapped offshore the Palomares margin in both tectonic regime and timing.

The N10°E transpressive faults of the Palomares margin offshore (e.g., positive flower structure imaged in line TM23) may represent the Plio-Quaternary southward propagation of the Palomares sinistral fault zone on land that initiated its activity during the latemost Tortonian (Figure 13). However, our data about the southward continuation of the Palomares fault system offshore are not conclusive.

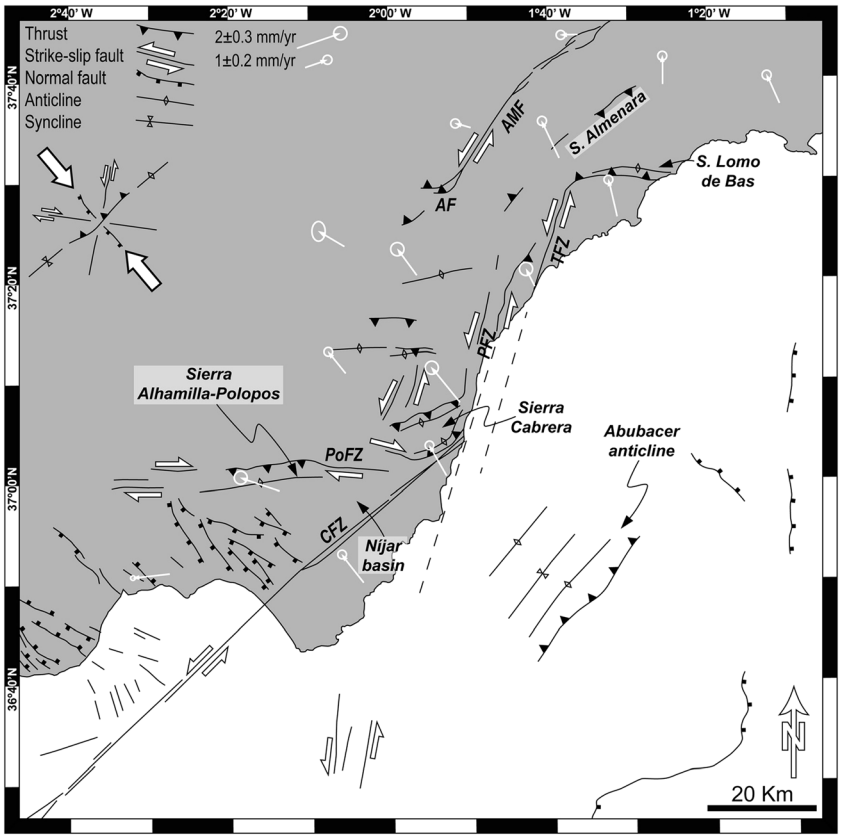

Figure 13. Structural sketch of the Palomares margin both onshore and offshore where the GPS geodetic data [*Echeverria et al.*, 2013] and the main tectonic structures active during the Quaternary are shown: the Albox fault (AF), the Alhama de Murcia fault (AMF), the Carboneras fault zone (CFZ), the Palomares fault zone (PFZ), the Polopos fault zone (PoFZ), and the Terreros fault zone (TFZ) (see Figure 1 for location) [*Booth-Rea et al.*, 2004a, 2004b; *Masana et al.*, 2004; *Marín-Lechado et al.*, 2005; *Masana et al.*, 2005; *Gràcia et al.*, 2006; *Pedrera et al.*, 2006, 2009; *Sanz de Galdeano et al.*, 2010; *Booth-Rea et al.*, 2012; *Giaconia et al.*, 2012a, 2012b; *Pedrera et al.*, 2012; *Giaconia et al.*, 2013]. The set of structures is consistent with the present stress field and fits in an oblique convergence model where a NW-SE trending shortening affects the NNE-SSW oriented Palomares margin. Strike-slip faults (e.g., PFZ, PoFZ, and TFZ) partition and transfer the deformation among en echelon thrusts and folds where shortening is mainly absorbed (e.g., Sierra Almenara, Sierra Cabrera, and Sierra Alhamilla).

During oblique convergence, shortening is mainly absorbed by en echelon thrusts and folds connected by strike-slip faults that partition the deformation, as described in other more evolved orogenic systems like the Zagros thrust-fold belt [*Vernant and Chery*, 2006; *Malekzade et al.*, 2007]. The Palomares and Terreros sinistral fault systems transfer shortening at Sierra Almenara and Lomo de Bas to the Sierra Cabrera at the south (Figure 14), while the dextral Polopos fault zone transfers shortening between Sierra Alhamilla to the west and Sierra Cabrera to the east (Figure 13) [*Giaconia et al.*, 2012a, 2012b, 2013]. The GPS displacement vector measured at the Sierra Cabrera anticlinorium is significantly larger than measurements to the north, indicating that the reverse faults that bound the anticlinorium are absorbing an important amount of the Africa-Iberia convergence in the region (Figure 13). Similarly, further east, the GPS displacement vectors decrease stepwise toward the north after the main active shortening structures, namely, the Lomo de Bas and Sierra Almenara reverse faults and the Alhama de Murcia sinistral reverse fault. The sinistral Palomares fault system partitions the deformation between the above shortening structures, having a smaller displacement vector that is oriented NNW-ward, congruent to the kinematics of the fault zone. Offshore, a large portion of the Africa-Iberia convergence is absorbed by the Abubacer N40°E thrust system and associated folds.

5.3. The Palomares Margin in the Tectonic Evolution of the Western Mediterranean

The continent to ocean transition between the Alboran and Algero-Balearic basins at the Palomares margin does not show the typical passive margin basement morphology with tilted blocks that have been recognized at nonvolcanic passive margins like the western Iberian one [e.g., *Reston et al.*, 2007] or at the

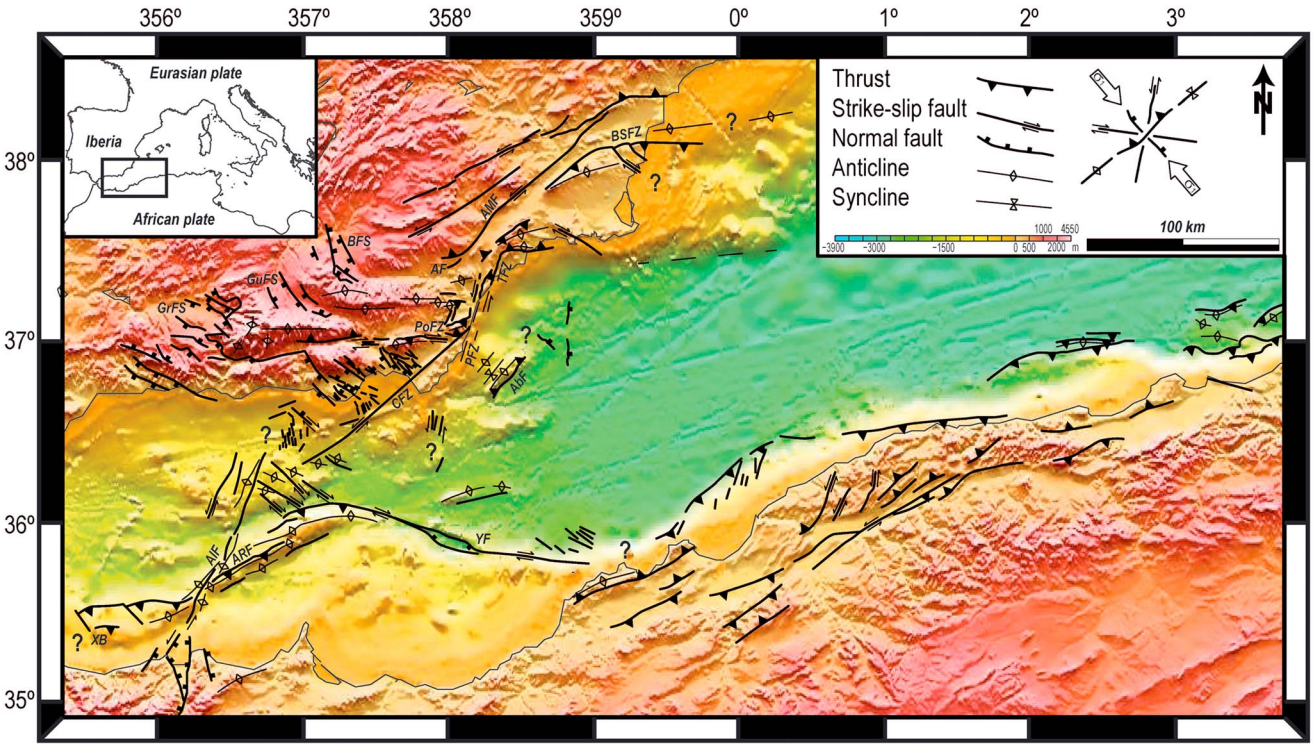

Figure 14. Main tectonic structures associated to the late Miocene (post latemost Tortonian) to present-day compressional tectonic inversion of the Betics, Rif, Alboran, and Algero-Balearic basins, both onshore and offshore. The fault traces and kinematic data are taken from previous authors [*Martínez-Díaz et al.*, 2002; *Booth-Rea et al.*, 2004a, 2004b; *Masana et al.*, 2004; *Booth-Rea et al.*, 2005; *Marín-Lechado et al.*, 2005; *Masana et al.*, 2005; *Domzig et al.*, 2006; *Gràcia et al.*, 2006; *Pedrera et al.*, 2006; *Moreno et al.*, 2008; *Pedrera et al.*, 2009; *Sanz de Galdeano et al.*, 2010; *Gràcia et al.*, 2011; *Alfaro et al.*, 2012; *Pedrera et al.*, 2012; *Perea et al.*, 2012; *Sanz de Galdeano et al.*, 2012; *Giaconia et al.*, 2013; *Maillard and Mauffret*, 2013; *Martínez-García et al.*, 2013; *d'Acremont et al.*, 2014]. AbF, Abubacer fault; AlF, Al-Idrisi fault; AMF, Alhama de Murcia fault; ARF, Alboran Ridge fault, BFS, Baza basin fault system, BSFZ, Bajo Segura fault zone; CFZ, Carboneras fault zone; GrFS, Granada basin fault system; GuFS, Guadix basin fault system; PFZ, Palomares fault zone; PoFZ, Polopos fault zone; TFZ; Terreros fault zone; XB, Xauen bank; YF, Yusuf fault. Question marks are zones where the lateral continuity of tectonic structures is unknown and needs further tectonic mapping.

Algerian margin (along S2 line) [*Medaouri et al.*, 2014] because here extension has been accounted by magmatic and volcanic activity during the Serravallian to Messinian. The important magmatic accretion at the Palomares margin is probably related to the late Miocene detachment of the lithospheric mantle under the eastern Betics, leading to edge delamination under the continental margin [e.g., *Duggen et al.*, 2003, 2004; *Booth-Rea et al.*, 2007]. Important transform and extensional transfer faults developed in this setting, like the Alpujarras dextral fault, the Carboneras sinistral fault, or the Yusuf dextral fault [*Martinez-Martinez et al.*, 2006b; *Rutter et al.*, 2012; *Giaconia et al.*, 2014]. These faults separate different tectonic extensional domains (core complexes, tilted blocks, crustal thinning, and magmatic accretion) to accommodate the westward migration of the slab beneath the Alboran region [*Giaconia et al.*, 2014]. Otherwise, the different tectonic styles of the transition could be due to transcurrent faults that separate and accommodate differential extension among different tectonic domains as the Carboneras and Yusuf faults. However, these two hypotheses are not necessarily exclusive considering the evolution from generalized extension before the latest Miocene to late transcurrent inversion of the basin since then. Although strike-slip faults at crustal level could be the shallower expression of deep-mantle geodynamic mechanisms (e.g., slab rollback, slab tearing/detachment, and edge delamination) and subduction transform edge propagator faults, these faults would have been reused later during contractive inversion.

Pure shortening and transpressive structures at the Palomares margin offshore are consistent with structures mapped onshore in the southeastern Betics and offshore at the Algerian margin, in both tectonic regime and timing. After middle-late Miocene E-W back-arc extension that generated the Algero-Balearic basin (16–8 Ma) [*Mauffret et al.*, 2004; *Booth-Rea et al.*, 2007], inversion of the Algerian margin occurred during the late Miocene (about 7–5 Ma) and has continued to present time [*Deverchere et al.*, 2005; *Domzig et al.*, 2006; *Mauffret*, 2007; *Billi et al.*, 2011]. Tectonic inversion reactivated S verging thrusts onshore the Algerian margin in

the Tortonian and produced new N verging thrusts near the continent to ocean transition offshore in the central and eastern Algerian margin since the Pliocene [*Deverchere et al.*, 2005; *Domzig et al.*, 2006; *Mauffret*, 2007; *Kherroubi et al.*, 2009; *Yelles et al.*, 2009; *Strzerzynski et al.*, 2010]. These structures cut the basement and fold late Tortonian-Messinian sediments and Plio-Quaternary sediments that show fold-onlapping growth strata [*Deverchere et al.*, 2005; *Domzig et al.*, 2006; *Kherroubi et al.*, 2009; *Billi et al.*, 2011]. The present tectonic activity is indicated by historical and instrumentally recorded thrust mechanism earthquakes and GPS geodetic displacement data [*Mauffret*, 2007; *Serpelloni et al.*, 2007; *Strzerzynski et al.*, 2010].

The Alboran ridge and Al-Idrisi faults in the East Alboran basin are structures kinematically equivalent to those of the Palomares margin. Although, in this case, the origin of these structures is younger, after the Messinian (5.33–4.57 Ma) [*Campos et al.*, 1992; *Martínez-García et al.*, 2013; *d'Acremont et al.*, 2014]. The N105°E Yusuf dextral fault that merges westward with the N60°E Alboran ridge reverse fault (Figure 14) cuts and folds the Plio-Quaternary sediments (e.g., the Yusuf and Alboran Ridge anticlines and the Yusuf Basin syncline). This fault system is cut by the N25°E Al-Idrisi sinistral fault toward the west that also shows Plio-Quaternary growth strata (Figure 14) [*Martínez-García et al.*, 2013; *d'Acremont et al.*, 2014]. However, at the west Alboran basin, the mid-Tortonian unconformity R3, together with the isolation of small basins [*Rodríguez Fernández et al.*, 1999; *Medaouri et al.*, 2014], has been interpreted as being produced by the tectonic uplift related to the inversion of the basin [*Bourgois et al.*, 1992; *Woodside and Maldonado*, 1992; *Chalouan et al.*, 1997; *Comas et al.*, 1999; *Soto et al.*, 2010]. However, no tectonic structure has been identified that could cause such tectonic inversion of the basin. Thus, the mid-Tortonian unconformity could be related to other processes like extension as documented offshore at the east Alboran basin [*Booth-Rea et al.*, 2007] or on land at the Betics [e.g., *Lonergan and Schreiber*, 1993; *Booth-Rea et al.*, 2004b; *Meijninger and Vissers*, 2006; *Giaconia et al.*, 2014]. We interpret that the presently active tectonic inversion of the Western Mediterranean started about 7 Ma near the Palomares and Algerian margins and most probably migrated westward at the western Algerian and the Moroccan margins by the development of the Alboran ridge and Al-Idrisi fault system about 5 Ma. Such a space-time evolution of the Western Mediterranean inversion indicates the development of a new transpressional plate boundary along the southern margin of the Algero-Balearic and Alboran basins that is propagating westward in response to the ongoing Eurasia-Africa plate convergence. The tip line of this newly developing plate boundary occurs along the Xauen bank at the southern margin of the West Alboran basin (Figure 14).

6. Conclusions

The MCS lines show the absence of a typical fault block structure across the continent to ocean transition of the Algero-Balearic basin at the Palomares margin. The extension and formation of the margin were largely accounted by important magmatic and volcanic activity during the Serravallian to Messinian, with tectonic thinning of a preexisting crust being possibly comparatively minor in the architecture of the region.

The integrated interpretation of the MCS images, parametric subbottom profiles, and bathymetric data indicates that the Palomares margin was later inverted from latemost Tortonian until present day. The inversion structures are N40–50°E reverse faults and folds (e.g., the Abubacer and Sierra Cabrera antiformal ridge and associated reverse faults) and N10°E sinistral strike-slip faults (e.g., Palomares-type faults) that crop out both onshore and offshore. The Abubacer reverse fault shows a planar geometry until its detachment close to the brittle-ductile transition at approximately 10 km depth and accommodates up to 1.5 km displacement.

The kinematics of tectonic structures both onshore and offshore the Palomares margin is consistent with the NW-SE present stress field. These structures fit in an oblique convergence model where NW-SE shortening is partitioned between en echelon reverse faults and associated folds (e.g., the N40–50°E striking Abubacer and Sierra Cabrera antiformal ridges and associated reverse faults) and strike-slip faults along a NNE-SSW margin (e.g., the sinistral N10°E striking Palomares and Terreros fault zones or the dextral N110–120°E Polopos fault zone). The strike-slip faults transfer deformation between shortening structures where most convergence is absorbed.

Tectonic inversion of the Palomares margin initiated during the latemost Tortonian to Messinian, coeval to structures observed along the Algerian margin and older with respect to the western Algerian and Morocco margins where inversion started in the Pliocene. Thus, the compressional inversion of the

Western Mediterranean is developing a new transpressive plate boundary at the southern margins of the Algero-Balearic and Alboran basins. This plate boundary has propagated westward from the Algerian margin approximately 7 Ma to the Alboran Ridge about 5 Ma, extending to the Xauen bank at the southern margin of the Western Alboran basin.

Acknowledgments

The seismic data were obtained in the frame of the European Science Foundation TopoEurope Project funded by the Spanish Ministry of Science and Innovation as TOPOMED CGL2008-03474-E project. The authors were supported by research group RNM148 (Junta de Andalucía), research group 2014 SGR 940 (Generalitat de Catalunya), and research projects CGL2011-29920, CSD2006-00041 TOPOIBERIA CONSOLIDER-INGENIO2010, CTM2007-66179-C02-01/MAR, CGL2011-30005-C02-02 SHAKE, and the CTM2011-30400-C02-01 HADES Project from the Spanish Ministry of Science and Innovation. We also acknowledge funding from the MICINN through the "Ramon y Cajal" (R. Bartolome) and Juan de la Cierva (H. Perea) programs. Our grateful thanks to the captain, crew, and UTM-CSIC technical staff onboard the R/V *Sarmiento de Gamboa*, during the TOPOMED-GASSIS cruise. We thank Laurent Jolivet, Damien do Couto, and other anonymous reviewers for their comments that helped improve the manuscript.

References

Aguirre, J. (1998), El Plioceno del SE de la Península Ibérica (provincia de Almería). Síntesis estratigráfica, sedimentaria, bioestratigráfica y paleogeográfica, *Rev. Soc. Geol. Esp.*, *11*, 295–315.

Aguirre, J., and I. M. Sánchez-Almazo (2004), The Messinian post-evaporitic deposits of the Gafares area (Almería-Níjar basin, SE Spain). A new view of the "Lago-Mare" facies, *Sediment. Geol.*, *168*(1–2), 71–95, doi:10.1016/j.sedgeo.2004.03.004.

Alfaro, P., R. Bartolomé, M. J. Borque, A. Estévez, J. García-Mayordomo, F. J. García-Tortosa, A. J. Gil, E. Gràcia, C. Lo Iacono, and H. Perea (2012), The Bajo Segura Fault Zone: Active blind thrusting in the Eastern Betic Cordillera (SE Spain), *J. Ib. Geol.*, *38*, 271–284.

Augier, R. (2004), Evolution tardi-orogénique des Cordillères Bétiques (Espagne): Apports d'une étude intégrée, Université Pierre et Marie Curie-Paris VI.

Azañón, J. M., A. Crespo-Blanc, and V. García-Dueñas (1997), Continental collision, crustal thinning and nappe-forming during the pre-Miocene evolution of the Alpujárride Complex (Alborán Domain, Betics), *J. Struct. Geol.*, *19*, 1055–1071.

Balanyá, J. C., V. García-Dueñas, J. M. Azañón, and M. Sánchez-Gómez (1997), Alternating contractional and extensional events in the Alpujarride nappes of the Alboran Domain (Betics, Gibraltar Arc), *Tectonics*, *16*(2), 226–238, doi:10.1029/96TC03871.

Ballesteros, M., J. Rivera, A. Muñoz, A. Muñoz-Martín, J. Acosta, A. Carbó, and E. Uchupi (2008), Alboran Basin, southern Spain—Part II: Neogene tectonic implications for the orogenic float model, *Mar. Pet. Geol.*, *25*(1), 75–101, doi:10.1016/j.marpetgeo.2007.05.004.

Bell, J. W., F. Amelung, and G. C. P. King (1997), Preliminary late Quaternary slip history of the Carboneras fault, southeastern Spain, *J. Geodyn.*, *24*, 51–66.

Billi, A., C. Faccenna, O. Bellier, L. Minelli, G. Neri, C. Piromallo, D. Presti, D. Scrocca, and E. Serpelloni (2011), Recent tectonic reorganization of the Nubia-Eurasia convergent boundary heading for the closure of the western Mediterranean, *Bull. Soc. Geol. Fr.*, *182*(4), 279–303.

Booth-Rea, G., J. M. Azáñon, B. Goffe, O. Vidal, and J. M. Martínez-Martínez (2002), High-pressure, low-temperature metamorphism in Alpujarride units of southeastern Betics (Spain), *C. R. Geosci.*, *334*(11), 857–865.

Booth-Rea, G., J. M. Azañón, A. Azor, and V. García-Dueñas (2004a), Influence of strike-slip fault segmentation on drainage evolution and topography. A case study: The Palomares fault zone (southeastern Betics, Spain), *J. Struct. Geol.*, *26*(9), 1615–1632.

Booth-Rea, G., J. M. Azañón, and V. García-Dueñas (2004b), Extensional tectonics in the northeastern Betics (SE Spain): Case study of extension in a multilayered upper crust with contrasting rheologies, *J. Struct. Geol.*, *26*, 2039–2058.

Booth-Rea, G., J. M. Azañón, J. M. Martínez-Martínez, O. Vidal, and V. García-Dueñas (2005), Contrasting structural and P-T evolutions of tectonic units in the southeastern Betics: Key for understanding the exhumation of the Alboran Domain HP/LT crustal rocks (Western Mediterranean), *Tectonics*, *24*, TC2009, doi:10.1029/2004TC001640.

Booth-Rea, G., C. Ranero, J. M. Martínez-Martínez, and I. Grevemeyer (2007), Crustal types and Tertiary tectonic evolution of the Alborán sea, western Mediterranean, *Geochem. Geophys. Geosyst.*, *8*, Q10005, doi:10.1029/2007GC001639.

Booth-Rea, G., F. Giaconia, J. M. Martínez-Martínez, and J. M. Azañón (2012), The Almenara detachment (southeastern Betics), *GeoTemas*, *13*, 1615–1618.

Bourgois, J., A. Mauffret, A. Ammar, and A. Demnati (1992), Multichannel seismic data Imaging of inversion tectonics of the Alboran Ridge (western Mediterranean-Sea), *Geo Mar. Lett.*, *12*(2–3), 117–122, doi:10.1007/Bf02084921.

Bousquet, J. C. (1979), Quaternary strike-slip faults in southeastern Spain, *Tectonophysics*, *52*, 277–286.

Braga, C., J. M. Martín, and C. Quesada (2003), Patterns and average rates of late Neogene-recent uplift of the Betic Cordillera, SE Spain, *Geomorphology*, *50*, 3–26.

Briand, F. (2008), The Messinian Salinity Crisis from mega-deposits to microbiology—A consensus report, paper presented at CIESM Workshop Monographs, no. 33, Monaco, 168.

Campos, J., A. Maldonado, and A. C. Campillo (1992), Post-Messinian evolutional patterns of the Central Alboran Sea, *Geo Mar. Lett.*, *12*(2–3), 173–178, doi:10.1007/Bf02084929.

Chalouan, A., S. Rachida, A. Michard, and A. W. Bally (1997), Neogene tectonic evolution of the southwestern Alboran basin as inferred from seismic data off Morocco, *AAPG Bull.*, *81*(7), 1161–1184.

CIESM (2008), The Messinian Salinity Crisis from mega-deposits to microbiology—A consensus report, in CEISM Workshop Monographs, edited by F. Briand, p. 168, Monaco.

Clauzon, G., J.-P. Suc, F. Gautier, A. Berger, and M.-F. Loutre (1996), Alternate interpretation of the Messinian salinity crisis: Controversy resolved?, *Geology*, *24*(4), 363–366, doi:10.1130/0091-7613(1996)024<0363:aiotms>2.3.co;2.

Clauzon, G., et al. (2015), New insights on the Sorbas Basin (SE Spain): The onshore reference of the Messinian Salinity Crisis, *Mar. Pet. Geol.*, doi:10.1016/j.marpetgeo.2015.02.016.

Comas, M. C., V. García Dueñas, and M. J. Jurado (1992), Neogene tectonic evolution of the Alboran Sea from MCS data, *Geo Mar. Lett.*, *12*, 157–164.

Comas, M. C., J. J. Dañobeitia, J. Alvárez Marrón, and J. I. Soto (1997), Crustal reflections and structure in the Alboran Basin. Preliminary results of the ESCI-Alborán survey, *Rev. Soc. Geol. Esp.*, *8*(4), 529–542.

Comas, M. C., J. P. Platt, J. I. Soto, and A. B. Watts (1999), The origin and tectonic history of the Alborán basin: Insights from leg 161 results, in *Proceedings of the Ocean Drilling Program, Scientific Results*, edited by R. Zahan, M. C. Comas, and A. Klaus, pp. 555–579, Ocean Drilling Program, Collage Station, Tex.

Coulon, C., M. Mergatsi, S. Fourcade, R. C. Maury, H. Bellon, A. Louni-Hacini, J. Cotten, A. Coutelle, and D. Hermitte (2002), Post-collisional transition from calc-alkaline to alkaline volcanism during the Neogene in Oranie (Algeria): Magmatic expression of a slab breakoff, *Lithos*, *62*, 87–110.

d'Acremont, E., et al. (2014), High-resolution imagery of active faulting offshore Al Hoceima, Northern Morocco, *Tectonophysics*, *632*, 160–166, doi:10.1016/j.tecto.2014.06.008.

Deverchere, J., et al. (2005), Active thrust faulting offshore Boumerdes, Algeria, and its relations to the 2003 M_w 6.9 earthquake, *Geophys. Res. Lett.*, *32*, L04311, doi:10.1029/2004GL021646.

Do Couto, D., C. Gumiaux, R. Augier, N. Lebret, N. Folcher, G. Jouannic, L. Jolivet, J.-P. Suc, and C. Gorini (2014a), Tectonic inversion of an asymmetric graben: Insights from a combined field and gravity survey in the Sorbas basin, *Tectonics*, *33*, 1360–1385, doi:10.1002/2013tc003458.

Do Couto, D., S.-M. Popescu, J.-P. Suc, M. C. Melinte-Dobrinescu, N. Barhoun, C. Gorini, L. Jolivet, J. Poort, G. Jouannic, and J.-L. Auxietre (2014b), Lago Mare and the Messinian Salinity Crisis: Evidence from the Alboran Sea (S. Spain), *Mar. Pet. Geol.*, *52*, 57–76, doi:10.1016/j.marpetgeo.2014.01.018.

Domzig, A., et al. (2006), Searching for the Africa-Eurasia Miocene boundary offshore western Algeria (MARADJA'03 cruise), *C. R. Geosci.*, *338*(1–2), 80–91.

Driussi, O., A. Maillard, D. Ochoa, J. Lofi, F. Chanier, V. Gaullier, A. Briais, F. Sage, F. Sierro, and M. Garcia (2014), Messinian Salinity Crisis deposits widespread over the Balearic Promontory: Insights from new high-resolution seismic data, *Mar. Pet. Geol.*, doi:10.1016/j.marpetgeo.2014.09.008.

Duggen, S., K. Hoernle, P. van den Bogaard, L. Rupke, and J. Phipps Morgan (2003), Deep roots of the Messinian salinity crisis, *Nature*, *422*, 602–606.

Duggen, S., K. Hoernle, P. van den Bogaard, and C. Harris (2004), The role of subduction in forming the western Mediterranean and causing the Messinian Salinity Crisis, *Earth Planet. Sci. Lett.*, *218*, 91–108.

Duggen, S., K. Hoernle, P. Van den Bogaard, and D. Garbe-Schonberg (2005), Post-collisional transition from subduction- to intraplate-type magmatism in the Westernmost Mediterranean: Evidence for continental-edge delamination of subcontinental lithosphere, *J. Petrol.*, *46*(6), 1155–1201.

Duggen, S., K. Hoernle, A. Klügel, J. Geldmacher, M. Thirlwall, F. Hauff, D. Lowry, and N. Oates (2008), Geochemical zonation of the Miocene Alborán Basin volcanism (westernmost Mediterranean): Geodynamic implications, *Contrib. Mineral. Petrol.*, *156*, 577–593.

Durand-Delga, M., P. Rossi, P. Olivier, and D. Puglisi (2000), Situation structurale et nature ophiolitique des roches basiques jurassiques associées aux flyschs maghrébins du Rif (Maroc) et de Sicile (Italie), *C. R. Acad. Sci. Paris*, *331*, 29–38.

Echeverria, A., G. Khazaradze, E. Asensio, J. Gárate, J. M. Dávila, and E. Suriñach (2013), Crustal deformation in eastern Betics from CuaTeNeo GPS network, *Tectonophysics*, *608*, 600–612, doi:10.1016/j.tecto.2013.08.020.

El Bakkali, S., A. Gourgaud, J. L. Bourdier, H. Bellon, and N. Gundogdu (1998), Post-collision Neogene volcanism of the Eastern Rif (Morocco): Magmatic evolution trough time, *Lithos*, *45*, 523–543.

Epard, J. L., and R. H. Groshong (1993), Excess area and depth to detachment, *AAPG Bull.*, *77*, 1291–1302.

Faccenna, C., C. Piromallo, A. Crespo-Blanc, L. Jolivet, and F. Rossetti (2004), Lateral slab deformation and the origin of the western Mediterranean arcs, *Tectonics*, *23*, TC1012, doi:10.1029/2002TC001488.

Fernández-Ibáñez, F., J. I. Soto, M. D. Zoback, and J. Morales (2007), Present-day stress field in the Gibraltar Arc (western Mediterranean), *J. Geophys. Res.*, *112*, B08404, doi:10.1029/2006JB004683.

Fortuin, A. R., and W. Krijgsman (2003), The Messinian of the Nijar Basin (SE Spain): Sedimentation, depositional environments and paleogeographic evolution, *Sediment. Geol.*, *160*(1–3), 213–242.

Galindo-Zaldívar, J., F. González-Lodeiro, and A. Jabaloy (1989), Progressive extensional shear structures in a detachment contact in the Western Sierra Nevada (Betic Cordilleras, Spain), *Geodinamica Acta*, *3*, 73–85.

García-Dueñas, V., and J. M. Martínez-Martínez (1988), Sobre el adelgazamiento mioceno del Dominio Cortical de Alborán, el Despegue Extensional de Filabres (Béticas orientales), *Geogaceta*, *5*, 53–55.

García-Dueñas, V., J. C. Balanyá, and J. M. Martínez-Martínez (1992), Miocene extensional detachments in the outcropping basement of the Northern Alboran Basin (Betics) and their tectonic implications, *Geo Mar. Lett.*, *12*, 88–95.

García-Meléndez, E., J. L. Goy, and C. Zazo (2003), Neotectonics and Plio-Quaternary landscape development within the eastern Huércal-Overa Basin (Betic Cordilleras, southeast Spain), *Geomorphology*, *50*(1–3), 111–133, doi:10.1016/S0169-555X(02)00210-6.

Gautier, F., G. Clauzon, J. P. Suc, J. Cravatte, and D. Violanti (1994), Age and duration of the Messinian salinity crisis, *C. R. Acad. Sci., Ser. IIa: Sci. Terre Planetes*, *318*(8), 1103–1109.

Giaconia, F., G. Booth-Rea, J. M. Martínez-Martínez, J. M. Azañón, and J. V. Pérez-Peña (2012a), Geomorphic analysis of the Sierra Cabrera, an active pop-up in the constrictional domain of conjugate strike-slip faults: The Palomares and Polopos fault zones (eastern Betics, SE Spain), *Tectonophysics*, *580*, 27–42, doi:10.1016/j.tecto.2012.08.028.

Giaconia, F., G. Booth-Rea, J. M. Martínez-Martínez, J. M. Azañón, J. V. Pérez-Peña, J. Pérez-Romero, and I. Villegas (2012b), Geomorphic evidence of active tectonics in the Sierra Alhamilla (eastern Betics, SE Spain), *Geomorphology*, *145–146*, 90–106, doi:10.1016/j.geomorph.2011.12.043.

Giaconia, F., G. Booth-Rea, J. M. Martínez-Martínez, J. M. Azañón, J. Pérez-Romero, and I. Villegas (2013), Mountain front migration and drainage captures related to fault segment linkage and growth: The Polopos transpressive fault zone (southeastern Betics, SE Spain), *J. Struct. Geol.*, *46*, 76–91, doi:10.1016/j.jsg.2012.10.005.

Giaconia, F., G. Booth-Rea, J. M. Martínez-Martínez, J. M. Azañón, F. Storti, and A. Artoni (2014), Heterogeneous extension and the role of transfer faults in the development of the southeastern Betic basins (SE Spain), *Tectonics*, *33*, 2467–2489, doi:10.1002/2014tc003681.

Gill, R. C. O., A. Aparicio, M. El Azzouzi, J. Hernandez, M. F. Thirlwall, J. Bourgois, and G. F. Marriner (2004), Depleted arc volcanism in the Alboran Sea and shoshonitic volcanism in Morocco: Geochemical and isotopic constraints on Neogene tectonic processes, *Lithos*, *78*(4), 363–388.

Goffé, B., A. Michard, V. García-Dueñas, F. González-Lodeiro, P. Monié, J. Campos, J. Galindo-Zaldívar, A. Jabaloy, J. M. Martínez-Martínez, and F. Simancas (1989), First evidence of high-pressure, low-temperature metamorphism in the Alpujarride nappes, Betic Cordillera (SE Spain), *Eur. J. Mineral.*, *1*, 139–142.

Gràcia, E., et al. (2006), Active faulting offshore SE Spain (Alboran Sea): Implications for earthquake hazard assessment in the Southern Iberian Margin, *Earth Planet. Sci. Lett.*, *241*(3–4), 734–749, doi:10.1016/j.epsl.2005.11.009.

Gràcia, E., C. R. Ranero, R. Bartolome, and GASSIS cruise party (2011), New seismic imaging across the Gibraltar Arc from the Alboran Sea to Gulf of Cadiz (South Iberia): First results of the TOPOMED-GASSIS cruise, in *Eos Trans AGU*, Fall meeting Suppl., San Francisco, Calif.

Gràcia, E., et al. (2012), Acoustic and seismic imaging of the Adra Fault (NE Alboran Sea): In search of the source of the 1910 Adra earthquake, *Nat. Hazard Earth Syst.*, *12*, 3255–3267, doi:10.5194/nhess-12-3255-2012.

Grevemeyer, I., and C. R. Ranero (2012), Seismic structure of crust formed by back-arc spreading, paper presented at AGU Fall Meeting, T53E-06.

Gutscher, M. A., J. Malod, J. P. Rehault, I. Contrucci, F. Klingelhoefer, L. Mendes-Victor, and W. Spakman (2002), Evidence for active subduction beneath Gibraltar, *Geology*, *30*, 1071–1074.

Hoernle, K., S. Duggen, J. Geldmacher, A. Klügel, and S. B. S. Party (2003), METEOR Cruise No. 51, Leg 1, Vulkosa: Vulcanismus Ostatlantik-Alboran in Meteor Berichte 03-1 Ostatlantik-Mittelmeer-Schwarzes Meer, Cruise No. 51, 2001, edited, GEOMAR Res. Cent., Kiel, Germany.

Hsü, K. J., W. B. F. Ryan, and M. B. Cita (1973), Late Miocene desiccation of the Mediterranean, *Nature*, *242*, 240–244.

Hsü, K., L. Montadert, D. Bernoulli, M. Cita, A. Erickson, R. Garrison, R. Kidd, F. Melières, C. Müller, and R. Wright (1977), History of the Messinian salinity crisis, *Nature*, *267*, 399–403.

Jurado, M., and M. Comas (1992), Well log interpretation and seismic character of the Cenozoic sequence in the northern Alboran Sea, *Geo Mar. Lett.*, *12*, 96–103.

Kherroubi, A., J. Deverchere, A. Yelles, B. Mercier de Lepinay, A. Domzig, A. Cattaneo, R. Bracene, V. Gaullier, and D. Graindorge (2009), Recent and active deformation pattern off the easternmost Algerian margin, Western Mediterranean Sea: New evidence for contractional tectonic reactivation, *Mar. Geol.*, *261*(1–4), 17–32, doi:10.1016/j.margeo.2008.05.016.

Krijgsman, W., F. J. Hilgen, I. Raffi, F. J. Sierro, and D. S. Wilson (1999), Chronology, causes and progression of the Messinian salinity crisis, *Nature*, *400*(6745), 652–655.

Krijgsman, W., A. R. Fortuin, F. J. Hilgen, and F. J. Sierro (2001), Astrochronology for the Messinian Sorbas basin (SE Spain) and orbital (precessional) forcing for evaporite cyclicity, *Sediment. Geol.*, *140*(1–2), 43–60.

Leuchters, W., I. Grevemeyer, C. R. Ranero, A. Villasenor, G. Booth-Rea, and J. Gallart (2011), Seismotectonics and seismic structure of the Alboran Sea, Western Mediterranean—Constraints from local earthquake monitoring and seismic refraction and wide-angle profiling, in Fall Meeting 2011, edited by A. G. Union.

Lofi, J., C. Gorini, S. Berné, G. Clauzon, A. Tadeu Dos Reis, W. B. F. Ryan, and M. S. Steckler (2005), Erosional processes and paleo-environmental changes in the Western Gulf of Lions (SW France) during the Messinian Salinity Crisis, *Mar. Geol.*, *217*(1–2), 1–30, doi:10.1016/j.margeo.2005.02.014.

Lofi, J., J. Déverchère, V. Gaullier, H. Gillet, C. Gorini, P. Guennoc, L. Loncke, A. Maillard, F. Sage, and I. Thinon (2011), Seismic atlas of the Messinian Salinity Crisis markers in the Mediterranean and Black Seas, *Mémoire Soc. Géol.*, *179*, 1–72.

Lonergan, L. (1993), Timing and kinematics of deformation in the Malaguide complex, internal zone of the Betic Cordillera, Southeast Spain, *Tectonics*, *12*(2), 460–476, doi:10.1029/92TC02507.

Lonergan, L., and B. C. Schreiber (1993), Proximal deposits at a fault-controlled basin margin, Upper Miocene, SE Spain, *J. Geol. Soc. London*, *150*, 719–727.

Lonergan, L., and N. White (1997), Origin of the Betic-Rif mountain belt, *Tectonics*, *16*(3), 504–522, doi:10.1029/96TC03937.

López Sánchez-Vizcaino, V., D. Rubatto, M. T. Gómez-Pugnaire, V. Trommsdorff, and O. Müntene (2001), Middle Miocene high-pressure metamorphism and fast exhumation of the Nevado-Filábride Complex, SE Spain, *Terra Nova*, *13*(5), 327–332.

Lugli, S., V. Manzi, M. Roveri, and C. B. Schreiber (2010), The Primary Lower Gypsum in the Mediterranean: A new facies interpretation for the first stage of the Messinian salinity crisis, *Palaeogeogr. Palaeoclimatol. Palaeoecol.*, *297*(1), 83–99, doi:10.1016/j.palaeo.2010.07.017.

Lujan, M., F. Storti, J. C. Balanya, A. Crespo-Blanc, and F. Rossetti (2003), Role of decollement material with different rheological properties in the structure of the Aljibe thrust imbricate (Flysch Trough, Gibraltar Arc): An analogue modelling approach, *J. Struct. Geol.*, *25*(6), 867–881.

Luján, M., A. Crespo-Blanc, and J. C. Balanyá (2006), The Flysch Trough thrust imbricate (Betic Cordillera): A key element of the Gibraltar Arc orogenic wedge, *Tectonics*, *25*, TC6001, doi:10.1029/2005TC001910.

Maillard, A., and A. Mauffret (2013), Structure and present-day compression in the offshore area between Alicante and Ibiza Island (Eastern Iberian Margin), *Tectonophysics*, *591*, 116–130.

Malekzade, Z., M. R. Abbassi, O. Bellier, and C. Authemayou (2007), Strain partitioning in West-Central Zagros fold and thrust belt: Implication for seismic hazard analysis, *J. Seismol. Earthquakes Eng.*, *9*, (No 3: Fall 2007), 85–98.

Manzi, V., R. Gennari, F. Hilgen, W. Krijgsman, S. Lugli, M. Roveri, and F. J. Sierro (2013), Age refinement of the Messinian salinity crisis onset in the Mediterranean, *Terra Nova*, *25*(4), 315–322, doi:10.1111/ter.12038.

Marín-Lechado, C., J. Galindo-Zaldivar, L. R. Rodriguez-Fernandez, I. Serrano, and A. Pedrera (2005), Active faults, seismicity and stresses in an internal boundary of a tectonic arc (Campo de Dalias and Nijar, southeastern Betic Cordilleras, Spain), *Tectonophysics*, *396*(1–2), 81–96.

Martín, J. M., and J. C. Braga (1994), Messinian events in the Sorbas Basin in southeastern Spain and their implications in the recent history of the Mediterranean, *Sediment. Geol.*, *90*, 257–268.

Martín, J. M., J. C. Braga, and C. Betzler (2003), Late Neogene-recent uplift of the Cabo de Gata volcanic province, Almeria, SE Spain, *Geomorphology*, *50*(1–3), 27–42, Pii S0169-555x(02)00206-4.

Martínez-Díaz, J. J., A. Rigo, L. Luis, R. Capote, J. L. Hernández-Enrile, E. Carreño, and M. Tsige (2002), Caracterización geológica y sismotectónica del terremoto de Mula (febrero de 1999, Mb: 4,8) mediante la utilización de datos geológicos, sismológicos y de interferometría de RADAR (INSAR), *Bol. Geol. Min.*, *113*, 22–33.

Martínez-García, P., M. Comas, J. I. Soto, L. Lonergan, and A. B. Watts (2013), Strike-slip tectonics and basin inversion in the Western Mediterranean: The post-Messinian evolution of the Alboran Sea, *Basin Res*, *25*, 1–27, doi:10.1111/bre.12005.

Martínez-Martínez, J. M., and J. M. Azañón (1997), Mode of extensional tectonics in the southeastern Betics (SE Spain). Implications for the tectonic evolution of the peri-Alborán orogenic system, *Tectonics*, *16*(2), 205–225, doi:10.1029/97TC00157.

Martínez-Martínez, J. M., J. I. Soto, and J. C. Balanyá (2002), Orthogonal folding of extensional detachments: Structure and origin of the Sierra Nevada elongated dome (Betics, SE Spain), *Tectonics*, *21*(3), 1012, doi:10.1029/2001TC001283.

Martínez-Martínez, J. M., G. Booth-Rea, and J. M. Azañón (2006a), Lateral interaction between metamorphic core complexes and less-extended, tilt-block domains: The Alpujarras strike-slip transfer Fault Zone (Betics, SE Spain), paper presented at EGU 2006 Geophysical Research Abstracts, 8, 02039.

Martínez-Martínez, J. M., G. Booth-Rea, J. M. Azañón, and F. Torcal (2006b), Active transfer fault zone linking a segmented extensional system (Betics, southern Spain): Insight into heterogeneous extension driven by edge delamination, *Tectonophysics*, *422*, 159–173, doi:10.1016/j.tecto.2006.06.001.

Masana, E., J. J. Martínez-Díaz, J. L. Hernández-Enrile, and P. Santanach (2004), The Alhama de Murcia fault (SE Spain), a seismogenic fault in a diffuse plate boundary: Seismotectonic implications for the Ibero-Magrebian region, *J. Geophys. Res.*, *109*, B01301, doi:10.1029/2002JB002359.

Masana, E., R. Pallas, H. Perea, M. Ortuno, C. Martínez-Díaz, E. García-Meléndez, and P. Santanach (2005), Large Holocene morphogenic earthquakes along the Albox fault, Betic Cordillera, Spain, *J. Geodyn.*, *40*, 119–133.

Mather, A. E. (1993), Basin inversion: Some consequences for drainage evolution and alluvial architecture, *Sedimentology*, *40*(6), 1069–1089, doi:10.1111/j.1365-3091.1993.tb01380.x.

Mauffret, A. (2007), The Northwestern (Maghreb) boundary of the Nubia (Africa) Plate, *Tectonophysics*, *429*(1–2), 21–44, doi:10.1016/j.tecto.2006.09.007.

Mauffret, A., A. Maldonado, and A. C. Campillo (1992), Tectonic framework of the Eastern Alboran and West Algerian Basins, Western Mediterranean, *Geo-Mar. Lett.*, *12*, 104–110.

Mauffret, A., D. Frizon de Lamotte, S. Lallemant, C. Gorini, and A. Maillard (2004), E-W opening of the Algerian Basin (Western Mediterranean), *Terra Nova*, *16*(5), 257–264, doi:10.1111/j.1365-3121.2004.00559.x.

Medaouri, M., J. Deverchere, D. Graindorge, R. Bracene, R. Badji, A. Ouabadi, K. Yelles-Chaouche, and F. Bendiab (2014), The transition from Alboran to Algerian basins (Western Mediterranean Sea): Chronostratigraphy, deep crustal structure and tectonic evolution at the rear of a narrow slab rollback system, *J. Geodyn.*, *77*, 186–205, doi:10.1016/j.jog.2014.01.003.

MEDIMAP GROUP, B. Loubrieu, and J. Mascle (2008), Morpho-bathymetry of the Mediterranean Sea, Map CIESM edition.

Meijninger, B. M. L. (2006), Late-orogenic extension and strike-slip deformation in the Neogene of southeastern Spain, Utrecht Univ.
Meijninger, B. M. L., and R. L. M. Vissers (2006), Miocene extensional basin development in the Betic Cordillera, SE Spain revealed through analysis of the Alhama de Murcia and Crevillente Faults, *Basin Res.*, *18*(4), 547–571, doi:10.1111/j.1365-2117.2006.00308.x.
Montenat, C., and P. Ott d'Estevou (1990), Eastern Betic Neogene basins—A review, in *Les Bassins Neogenes du Domaine Bétique Orientale (Espagne)*, edited by C. Montenat, pp. 9–15, Documents et Travaux IGAL, Paris.
Mora, M. (1993), *Tectonic and Sedimentary Analysis of the Huércal-Overa Region, SE Spain, Betic Cordillera*, Oxford Univ., Oxford England.
Moreno, X., E. Masana, E. Gràcia, C. Bartolome, and O. Piqué-Serra (2008), Estudio paleosismológico de la Falla de Carboneras: Evidencias tierra-mar de actividad tectónica reciente, *GeoTemas*, *10*, 1035–1038.
Muñoz, A., M. Ballesteros, I. Montoya, J. Rivera, J. Acosta, and E. Uchupi (2008), Alboran Basin, southern Spain—Part I: Geomorphology, *Mar. Pet. Geol.*, *25*, 59–73.
Omodeo Salé, S., R. Gennari, S. Lugli, V. Manzi, and M. Roveri (2012), Tectonic and climatic control on the Late Messinian sedimentary evolution of the Nijar Basin (Betic Cordillera, Southern Spain), *Basin Res*, *24*(3), 314–337, doi:10.1111/j.1365-2117.2011.00527.x.
Pedrera, A., C. Marín-Lechado, J. Galindo-Zaldívar, L. R. Rodríguez-Fernández, and A. Ruiz-Constán (2006), Fault and fold interaction during the development of the Neogene-Quaternary Almería-Níjar basin (SE Betic Cordilleras), *Geol. Soc. Spec. Publ.*, *262*, 217–230.
Pedrera, A., J. Galindo-Zaldivar, A. Ruiz-Bustos, J. Rodriguez-Fernandez, and A. Ruiz-Constan (2009), The role of small-scale fold and fault development in seismogenic zones: example of the western Huercal-Overa Basin (eastern Betic Cordillera, Spain), *J. Quat. Sci.*, *24*(6), 581–592, doi:10.1002/Jqs.1246.
Pedrera, A., J. Galindo-Zaldívar, A. Tello, and C. Marín-Lechado (2010), Intramontane basin development related to contractional and extensional structure interaction at the termination of a major sinistral fault: The Huércal-Overa Basin (Eastern Betic Cordillera), *J. Geodyn.*, *49*(5), 271–286, doi:10.1016/j.jog.2010.01.008.
Pedrera, A., J. Galindo-Zaldivar, C. Marin-Lechado, F. J. Garcia-Tortosa, P. Ruano, A. C. L. Garrido, J. M. Azanon, J. A. Pelaez, and F. Giaconia (2012), Recent and active faults and folds in the central-eastern internal zones of the Betic Cordillera, *J. Ib. Geol.*, *38*(1), 191–208, doi:10.5209/rev_JIGE.2012.v38.n1.39213.
Perea, H., E. Gràcia, P. Alfaro, R. Bartolomé, C. Lo Iacono, X. Moreno, E. Masana, and E.-S. Team (2012), Quaternary active tectonic structures in the offshore Bajo Segura basin (SE Iberian Peninsula-Mediterranean Sea), *Nat. Hazard Earth. Syst.*, *12*(10), 3151–3168, doi:10.5194/nhess-12-3151-2012.
Pesquer, D. A., I. Grevemeyer, C. R. Ranero, and J. Gallart (2008), Seismic structure of the passive continental margin of SE Spain and the SW Balearic promontory, western Mediterranean sea, in AGU Fall Meeting 2008, edited by E. Transactions, Abstract T43C-2053.
Platt, J., S. Allerton, A. Kirker, and E. Platzman (1995), Origin of the western Subbetic arc (South Spain)—Paleomagnetic and structural evidence, *J. Struct. Geol.*, *17*(6), 765–775.
Platt, J. P., and R. L. M. Vissers (1989), Extensional collapse of thickened continental lithosphere: A working hypothesis for the Alboran Sea and Gibraltar Arc, *Geology*, *17*, 540–543.
Platt, J. P., S. Allerton, A. Kirker, C. Mandeville, A. Mayfield, E. S. Platzman, and A. Rimi (2003), The ultimate arc: Differential displacement, oroclinal bending, and vertical axis rotation in the external Betic-Rif arc, *Tectonics*, *22*(3), doi:10.1029/2001TC001321.
Platt, J. P., S. P. Kelley, A. Carter, and M. Orozco (2005), Timing of tectonic events in the Alpujárride Complex, Betic Cordillera, southern Spain, *J. Geol. Soc. London*, *162*, 1–12.
Platt, J. P., R. Anczkiewicz, J. I. Soto, S. P. Kelley, and M. Thirlwall (2006), Early Miocene continental subduction and rapid exhumation in the Western Mediterranean, *Geology*, *34*(11), 981–984.
Ranero, C. R., and M. Perez-Gussinye (2010), Sequential faulting explains the asymmetry and extension discrepancy of conjugate margins, *Nature*, *468*(7321), 294–299. [Available at http://www.nature.com/nature/journal/v468/n7321/abs/nature09520.html#supplementary-information.]
Ranero, C. R., T. J. Reston, I. Belykh, and H. Gnibidenko (1997), Reflective oceanic crust formed at a fast-spreading center in the Pacific, *Geology*, *25*(6), 499–502.
Reston, T. J., C. R. Ranero, and I. Belykh (1999), The structure of Cretaceous oceanic crust of the NW Pacific: Constraints on processes at fast spreading centers, *J. Geophys. Res.*, *104*(B1), 629–644, doi:10.1029/98JB02640.
Reston, T. J., T. Leythaeuser, G. Booth-Rea, D. Sawyer, D. Klaeschen, and C. Long (2007), Movement along a low-angle normal fault: The S reflector west of Spain, *Geochem. Geophys. Geosyst.*, *8*, Q06002, doi:10.1029/2006GC001437.
Riding, R., J. C. Braga, M. J. Martín, and I. M. Sánchez Almazo (1998), Mediterranean Messinian Salinity Crisis: Constraints from a coeval marginal basin, Sorbas, Southeastern Spain, *Mar. Geol.*, *146*, 1–20.
Rodríguez Fernández, J., M. C. Comas, J. Soria, J. A. Martín Pérez, and J. I. Soto (1999), The sedimentary record of the Alboran Basin: An attempt at sedimentary sequence correlation and subsidence analysis, in *Proceedings of the Ocean Drilling Program, Scientific Results*, edited by R. Zahn, M. C. Comas, and A. Klaus, pp. 69–76.
Ruegg, G. (1964), Geologische onderzoekingen in het bekken van Sorbas, S Spanje, 64 pp., Amsterdam Geological Institute, Univ. of Amsterdam.
Rutter, E. H., D. R. Faulkner, and R. Burgess (2012), Structure and geological history of the Carboneras Fault Zone, SE Spain: Part of a stretching transform fault system, *J. Struct. Geol.*, *1–19*, doi:10.1016/j.jsg.2012.05.001.
Ryan, W., and J. E. A. Hsü (1973), Init. Repts. DSDP, 13 (Pts. 1 and 2), edited by U. S. G. P. Office, Washington, D. C.
Sanz de Galdeano, C., and J. A. Vera (1992), Stratigraphic record and palaeogeographical context of the Neogene basins in the Betic Cordillera, Spain, *Basin Res.*, *4*(1), 21–35.
Sanz de Galdeano, C., S. Shanov, J. Galindo-Zaldivar, A. Radulov, and G. Nikolov (2010), A new tectonic discontinuity in the Betic Cordillera deduced from active tectonics and seismicity in the Tabernas Basin, *J. Geodyn.*, *50*(2), 57–66, doi:10.1016/j.jog.2010.02.005.
Sanz de Galdeano, C., F. J. García-Tortosa, J. A. Peláez, P. Alfaro, J. M. Azañón, J. Galindo-Zaldívar, C. López Casado, A. C. López Garrido, J. Rodríguez-Fernández, and P. Ruano (2012), Main active faults in the Granada and Guadix-Baza Basins (Betic Cordillera), *J. Ib. Geol.*, *38*, 209–223.
Serpelloni, E., G. Vannucci, S. Pondrelli, A. Argnani, G. Casula, M. Anzidei, P. Baldi, and P. Gasperini (2007), Kinematics of the Western Africa-Eurasia plate boundary from focal mechanisms and GPS data, *Geophys. J. Int.*, *169*(3), 1180–1200, doi:10.1111/j.1365-246X.2007.03367.x.
Sierro, F. J., F. J. Hilgen, W. Krijgsman, and J. A. Flores (2001), The Abad composite (SE Spain): A Messinian reference section for the Mediterranean and the APTS, *Palaeogeogr. Palaeoclimatol. Palaeoecol.*, *168*(1–2), 141–169.
Soto, J. I., M. C. Comas, J. M. Azañón, J. M. Martínez-Martínez, M. Sánchez-Gómez, and B. C. T.-L. S. Party (2000), Structure of the Palomares and Mazarron margins (SE Spain), in *International Conference and Eight Post-Cruise Meeting of the Training-Trough-Research Programme*, edited by I. O. Commission, pp. 29, UNESCO 2000, Granada, Spain.
Soto, J. I., F. Fernandez-Ibanez, A. R. Talukder, and P. Martinez-Garcia (2010), Miocene shale tectonics in the northern Alboran Sea (western Mediterranean), in *Shale Tectonics*, vol. 93, edited by L. Wood, pp. 119–144, AAPG Memoir, Tulsa, Okla.
Spakman, W., and R. Wortel (2004), A tomographic view on Western Mediterranean geodynamics, in *The TRANSMED Atlas, the Mediterranean Region from Crust to Mantle*, edited by W. Cavazza et al., pp. 31–52, Springer, Berlin.

Stapel, G., R. Moeys, and C. Biermann (1996), Neogene evolution of the Sorbas basin (SE Spain) determined by paleostress analysis, *Tectonophysics*, *255*, 291–305.

Stich, D., C. J. Ammon, and J. Morales (2003), Moment tensor solutions for small and moderate earthquakes in the Ibero-Maghreb region, *J. Geophys. Res.*, *108*(B3), 2148, doi:10.1029/1202JB002057.

Stich, D., E. Serpelloni, F. de Lis Mancilla, and J. Morales (2006), Kinematics of the Iberia-Maghreb plate contact from seismic moment tensors and GPS observations, *Tectonophysics*, *426*(3–4), 295–317.

Stokes, M., and A. E. Mather (2000), Response of Plio-Pleistocene alluvial systems to tectonically induced base-level changes, Vera Basin, SE Spain, *J. Geol. Soc. London*, *157*, 303–316.

Strzerzynski, P., J. Deverchere, A. Cattaneo, A. Domzig, K. Yelles, B. M. de Lepinay, N. Babonneau, and A. Boudiaf (2010), Tectonic inheritance and Pliocene-Pleistocene inversion of the Algerian margin around Algiers: Insights from multibeam and seismic reflection data (vol 8, TC2008, 2010), *Tectonics*, *29*, TC3099, doi:10.1029/2010TC002716.

Turner, S. P., J. P. Platt, R. M. M. George, S. P. Kelley, D. G. Pearson, and G. M. Nowell (1999), Magmatism associated with orogenic collapse of the Betic-Alboran domain, SE Spain, *J. Petrol.*, *40*(6), 1011–1036.

Vernant, P., and J. Chery (2006), Mechanical modelling of oblique convergence in the Zagros, Iran, *Geophys. J. Int.*, *165*(3), 991–1002, doi:10.1111/j.1365-246X.2006.02900.x.

Völk, H. R. (1966), Geologie et stratigraphie du Bassin Neogene de Vera, Doctoral, inédita thesis, 121 pp., Universidad de Amsterdan.

Völk, H. R., and H. E. Rondeel (1964), Zur Gliederungdes des Juntertiars in becken von Vera, Sudspanien, *Geol. Minjbow*, *43*, 310–315.

Weijermars, R., T. B. Roep, B. Van den Eeckhout, G. Postma, and K. Kleverlaan (1985), Uplift history of a Betic fold nappe inferred from Neogene-Quaternary sedimentation and tectonics (in the Sierra Alhamilla and Almería, Sorbas and Tabernas Basins of the Betic Cordilleras, SE Spain), *Geol. Mijnbouw*, *64*, 397–411.

Woodside, J. M., and A. Maldonado (1992), Styles of compressional neotectonics in the Eastern Alboran Sea, *Geo Mar. Lett.*, *12*, 111–116.

Yelles, A., et al. (2009), Plio-Quaternary reactivation of the Neogene margin off NW Algiers, Algeria: The Khayr al Din bank, *Tectonophysics*, *475*(1), 98–116, doi:10.1016/j.tecto.2008.11.030.

Zeck, H. P. (1999), Alpine plate kinematics in the western Mediterranean: A westward-directed subduction regime followed by slab roll-back and slab detachment, *Geol. Soc. London, Spec. Publ.*, *156*(1), 109–120, doi:10.1144/gsl.sp.1999.156.01.07.